Coordination Chemistry Reviews, 9 (1972–1973) 275–310

X-RAY ABSORPTION EDGE SPECTROMETRY (XAES) AS APPLIED TO COORDINATION CHEMISTRY

U.C. SRIVASTAVA* and H.L. NIGAM
Chemistry Department, Allahabad University, Allahabad (India)
(Received February 1st, 1972)

CONTENTS

* Present address: Chemistry Department, C.M.P. College (Allahabad University), Allahabad (India).

ABBREVIATIONS

TPA	thiopropionic acid	$(et)_4$ dien	$HN[CH_2 \cdot CH_2 \cdot N(C_2H_5)_2]_2$
TMA	thiomalic acid	EW	edge width
TSA	thiosalicylic acid	en	ethylenediamine
TV	thiovanol	ATU	1-amino-2-thiourea
EA3CS	carboxymethyl-mercapto-succinic acid	DPDTP	diphenyldithiophosphinate
		INAP	isonitrosoacetato-phenonate
py	pyridine	l.f.s.e.	ligand field stabilization energy

A. INTRODUCTION

X-ray absorption edge spectrometry (XAES), i.e. the analysis of the spectrum of X-rays transmitted through matter, has recently shown promise of being adopted as a conventional tool for investigating problems in coordination chemistry. By virtue of the applicability of the technique, irrespective of the physical state of the matter investigated, and its direct dependence on the symmetry and energy of electronic states, the spectra have been of immense diagnostic value in providing information about the optical levels, which, for a coordination chemist, form the region of greatest interest. The reviews which have appeared earlier on the subject[7, 41, 66, 106] have mostly served as a supplement to emission spectroscopy. However, an independent review dealing exclusively with "the application of X-ray absorption spectroscopy to coordination chemistry" does not seem to have appeared in the literature. This defines precisely the aim of the present review. The review is also expected to contribute to the evolution of a systematic theory, which has also not yet been developed. To minimize the size of the text, experimental details have almost completely been ignored, and for such details relevant texts[20,27,103,127] may be consulted. No claim is made to the effect that the review is exhaustive with regard to references but every effort has been made to include up-to-date work on the most fundamental aspects of coordination chemistry, viz. the valency of the metal ion, the coordination symmetry, the bonding involved and finally the nature of the bond.

X-ray absorption spectra correspond to electronic transitions from inner electronic levels to outer unoccupied levels which are essentially the regions of interatomic orbital overlap. Within the limits of the resolution of the spectrographic set-up, therefore, the technique can be exploited to throw light on many stereochemical features of a complex, such as the bonding configuration, the ligand field symmetry, the valency of the central metal ion, etc. both in solution and in the solid state.

B. THE ENERGY REGIONS AND X-RAY ABSORPTION TRANSITIONS

The behaviour of the absorption coefficient around the absorption edge (the sharp discontinuity observed at a critical wavelength in the curve of absorption coefficient vs. wavelength in a particular region) of an element in a compound is determined, according to Coster and Kiestra[28,31], by: (*a*) the atomic character of the element at energies up to 40 eV higher than that of the main absorption edge (Kossel structure[57]); (*b*) the immediate surroundings in the region 40—150 eV, and (*c*) the whole crystal lattice in the

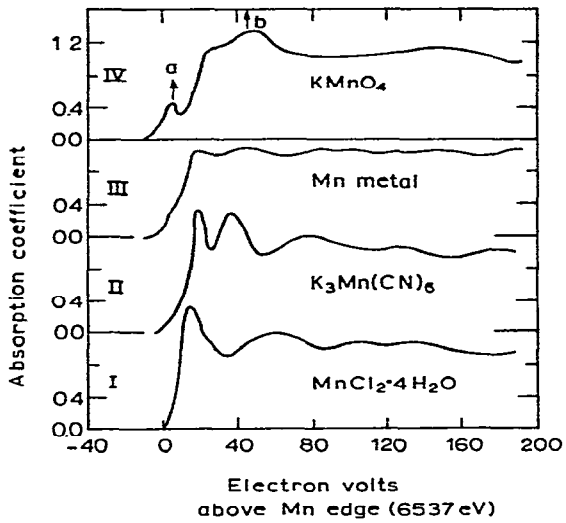

Fig. 1. *K*-absorption spectra of manganese in the metal and some compounds.

region beyond 150 eV (Kronig structure[59]). The electronic transitions (to optical levels) associated with X-ray absorption are allowed by the selection rule[100] $\Delta l = \pm 1$. In the case of coordination complexes, the transitions are decided by a number of considerations, including the symmetry and overlap of wave functions[38], and the covalent mixing parameters in occupied and unoccupied orbitals vis-à-vis the relative energies and intensities of absorption edge features[3,17].

(i) The low energy region

According to Mitchell and Beaman[72] the small maxima appearing to the long-wave side ot the main edge (the inflection point of the steep curve) are of considerable importance in the assignment of bonding orbitals. The appearance of these maxima are associated[72,110] with the presence or absence of an unfilled $4p$ shell (as, for example, in Van Nordstrand's Type IV spectra[128,129] (Fig. 1)). Thus this absorption in $Ni(CN)_4^{2-}$ has been attributed to the transition of a $1s$ electron into the low-lying $4p_z$ orbital (cf. the valence bond model) by Boke[22], Collet[26], Kauer[52] and Mitchell[73]. However, this view appears to be less convincing for the tetrahedral case involving sp^3 bonding, since, although the $4p$ level would be completely filled in this case, the low-energy absorption can still be observed, for instance[29,89,104] in $KMnO_4$ (Fig. 1). Hanson and Knight[43] have shown that as the $3d$ level becomes progressively filled, this low-energy absorption disappears, suggesting a $1s \rightarrow 3d$ quadrupole transition ($\Delta l = \pm 2$). The $3d$ band in Ni is about 4 eV wide[77] and can be resolved. As such the assignment of $1s \rightarrow 3d$ or $1s \rightarrow$ mixed $3d$–$4p_z$ to the low-energy maximum in $Ni(CN)_4^{2-}$ may not be ruled out. Vainshtein[126] has observed two small maxima in the $1s \rightarrow 3d$ region in the case of TiO_2,

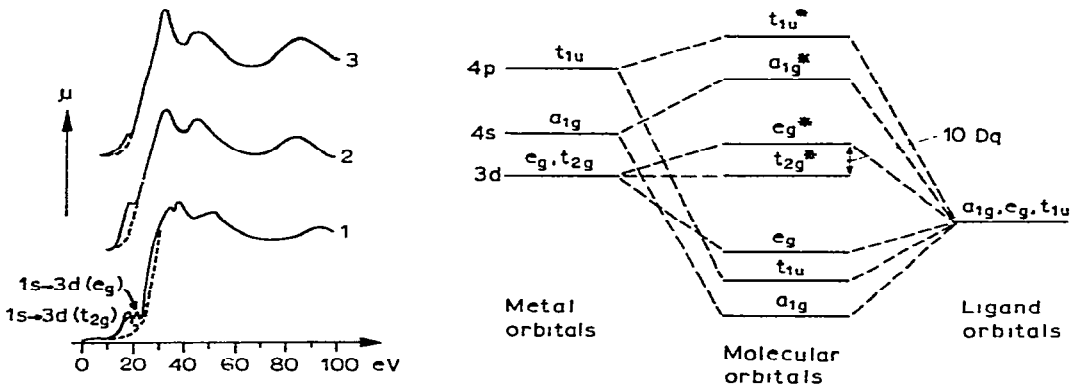

Fig. 2(a). *K*-absorption edge of Ti in TiO_2 (1); TiC (2); TiN (3).
Fig. 2(b). Simple MO energy level diagram for octahedral coordination.

and has attributed this to the splitting of the $3d$ orbitals into $3d(e_g)$ and $3d(t_{2g})$ (Fig. 2) under the influence of the crystal field due to the O^{2-} ion. Such a splitting of the low-energy absorption has also been observed[85] (Fig. 3) in the case of the *K*-absorption edge of cobalt in Co–TPA (thiopropionic acid) and Co–TV (thiovanol). The energy separation observed has been shown to be the same as the $10\,Dq$ values reported for these complexes[69,99]. Similarly, Cotton and Hanson[35] have designated such an absorption as $1s \rightarrow$ (partially vacant) $3d\ t_{2g}$ in $Na_3Cr(C_2O_4)_3$.

In complex systems involving low-lying π-orbitals, this low-energy absorption may result from the overlap of metal $3d$-orbitals of T_{2g} symmetry with ligand π-orbitals. Thus in the case of $K_3Fe(CN)_6$ and $Cr(CO)_6$, while Kauer[52] designated the low-lying maxima as $1s \rightarrow 4p$ (which are, however, filled), Cotton and Hanson[35] have preferred to attribute this to the transition of the $1s$ electron to those π-molecular orbitals which are ψ (ligand) ($\pi Pz + \psi\ 3d\ t_{2g}$). Similarly in $(NH_4)_3Co(NO_2)_6$ the transition is more probably due to molecular orbitals formed from metal $3d\ t_{2g}$ and empty antibonding $\pi\ B'_2$ orbitals of the NO_2^- ion. Some Cu^{II} complexes involving sulphur ligands in which the metal $3d$ orbitals are partially vacant also show this feature[81] (Fig. 4). A splitting of the $1s \rightarrow 3d$ absorption in the case of some cobalt complexes[85] (Fig. 3) has also been observed.

In the region between the main edge and the absorption maximum a shoulder may be observed, for instance[104] in K_2CrO_4. This shoulder is assigned[33] to a normally disallowed transition, $1s \rightarrow 4s$, in some copper complexes where it appears $\sim$10 eV below the main peak (Fig. 5). This is in general agreement with theory[13] (the energy difference between $3d^9\ 4s$ and $3d^9\ 4p$ in Zn^{II} being $\sim$10 eV[6]). The transition may become allowed as a result of mixing with ligand p-orbitals[38]. However, the low-energy shoulders observed (Fig. 4) in the case of Cu^{II}–thiosalicylic acid (TSA) and Cu^{II}–carboxymethylmercaptosuccinic acid (EA3CS) complexes (where $4s$ is filled) are assigned[81] to the $1s$–$4s^*$ (antibonding) transition.

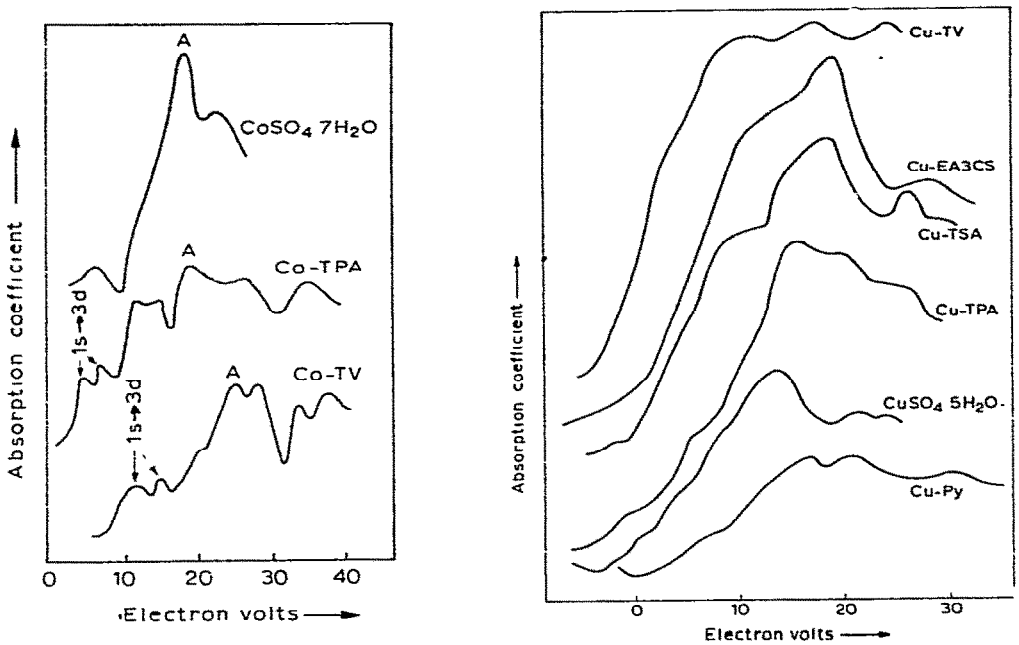

Fig. 3. *K*-absorption edge of cobalt in complexes having O_h and lower symmetries.

Fig. 4. *K*-absorption spectra of copper in complexes.

(ii) The principal absorption maximum

Quite recently, Bhide and Bhat[18] have shown that the absorption maximum of the yttrium *K* edge in Y^{3+} (aq.) is due to the excitation of a 1*s* electron into the 5*p* level, the theoretical $1s \rightarrow 5p$ energy difference of 4.139×10^{18} cps agreeing well with the observed value of 4.13×10^{18} cps. Earlier, the $1s \rightarrow 5p$ transition was also assigned to the main peak in $K_3Fe(CN)_6$ and $Cr(CO)_6$ (complexes of the first transition series) by Kauer[52]. However, Cotton and Hanson[35] have rightly contended that in these cases the absorption maximum corresponds more probably to the excitation of a 1*s* electron into those antibonding orbitals which are $(\psi_{\text{ligand}} - \psi_{4p})$, abbreviated as $1s \rightarrow 4p^*$ (antibonding). Mande and co-workers[65,110] have also concluded, both from theoretical and experimental investigations, that the *K*-absorption maximum, in the case of an octahedral complex of the first transition series, corresponds to the transition $1s \rightarrow 4p\ (t_{1u})^*$. In the second transition series, Barinskii[8] has assigned a transition $2p \rightarrow 4d$ to the L_{III} edge of molybdenum in $K_4Mo(CN)_8$ and $(NH_4)_2MoO_4$.

(iii) The Kossel region

Glen and Dod[38] have suggested that the second absorption maximum observed in the

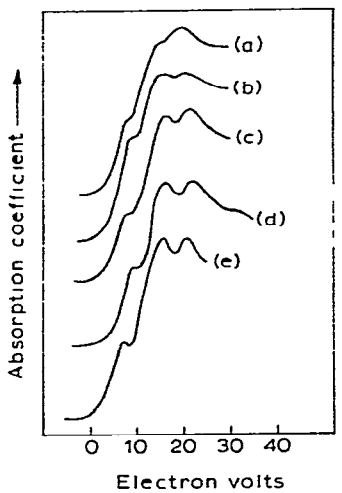

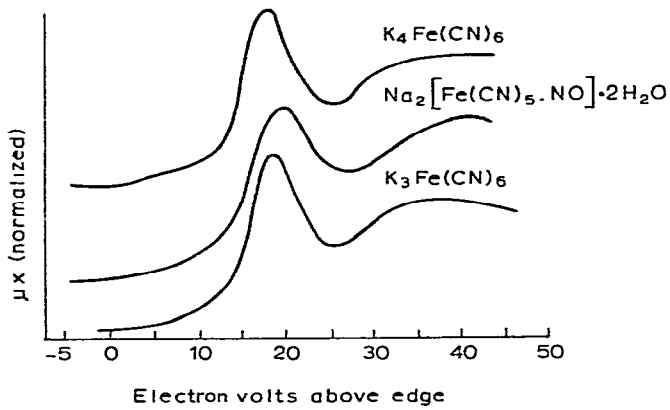

Fig. 5. *K*-absorption edges of some cupric complexes of D_{4h} or lower symmetry. (a) Cu(proline)$_2$ $2H_2O$; (b) $Cu(en)_2(NO_3)_2$; (c) $Cu(NH_3)_4SO_4 \cdot H_2O$; (d) $Cu(NH_3)_4(NO_3)_2$; (e) $Cu(NH_3)_4^{2+}$(aq.).

Fig. 6. *K*-absorption spectra of iron in some complexes.

K-spectra of ferri- and ferrocyanides (Fig. 6) may be attributed to the interaction of the 1*s* electron with the antibonding π levels of the cyanide ligand, in agreement with the calculations of Alexander and Gray[4]. Beaman and Bearden[14] have assigned the maxima subsequent to the main peak as $1s \rightarrow np$ ($n = 5, 6$ ... etc.) and have thereby shown that the 6*p* level is roughly 4 eV above 5*p* and the 7*p* level about 2 eV above 6*p* for Ni^{2+}, Cu^{2+} and Zn^{2+}. Bhide and Bhat[18] have suggested that the second absorption maximum (Fig. 7) in the *K*-spectra of Y^{3+} may be due to $1s \rightarrow 6p$ with contributions from 7*p* and higher energy levels, the calculated 5*p*–6*p* separation agreeing reasonably well with the observed separation.

C. EDGE SHIFT AND VALENCY OF THE METAL ION

The shift of the X-ray absorption edge due to chemical combination first observed by Bergengren[16] and later by others[2,25,27,61,118] has been shown to depend primarily on the valency of the element in question. The edge shift in general shows a marked increase with increasing oxidation state. Stelling[119] observed that in the case of sulphur, the edge shifted by about 0.46% in going from S^{2-} to S^{6+} compounds. Since the wave number is 20,000 kK, the shift of 90 kK is comparable to chemical bond energies.

(i) Shift in the position of the main edge

Boehm et al.[21] used the valency effect to show that cobalt in vitamin B_{12} is trivalent.

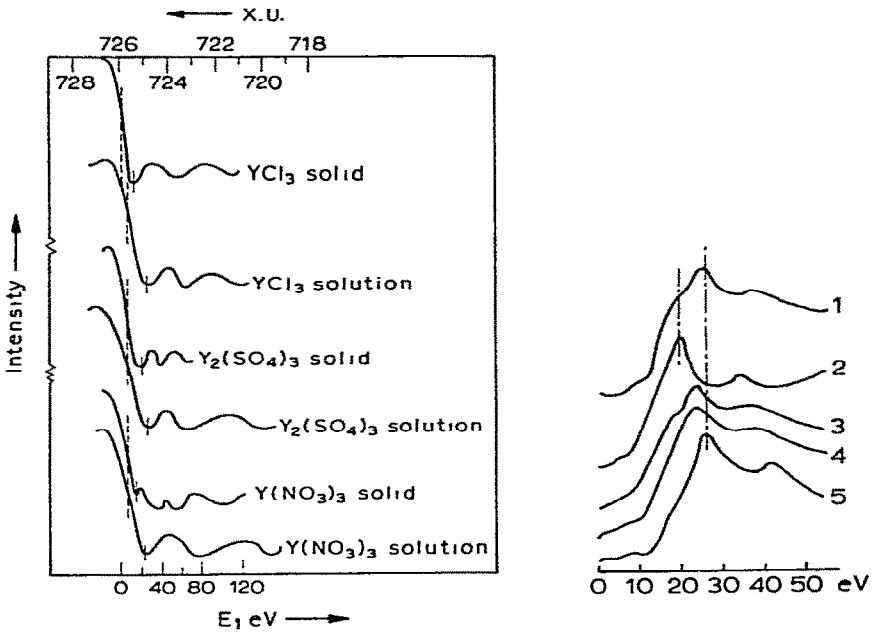

Fig. 7. *K*-absorption spectra of yttrium in compounds.

Fig. 8. *K*-absorption spectra of manganese in $CoMn_2O_4$ (1); MnO (2); Mn_3O_4 (3); Mn_2O_3 (4); MnO_2 (5).

Mande and Chetal[65] have similarly shown, by comparison with *K*-edge shifts in well known Co^{II} and Co^{III} compounds, that freshly prepared Co^{II}–thiomalic acid (TMA) complex[82] is oxidized to Co^{III} in air (Table 1). The energy difference between the *K* edges for Co^{II} and Co^{III}, ~4 eV, is in agreement with the values obtained by Agarwal and Nigam[2] and by the present authors[85], the latter involving some sulphur ligand complexes. Miller[67] has similarly established the divalency of copper in the spinel $CuMn_2O_4$. The edge shift of copper in $Cu_2Fe(CN)_6$ is also consistent[133] with its valency in the complex. However, the *K* edge shifts of the metal ion in some cobalt complexes and in the ferro- and ferricyanides reported by Obashi[89] are less convincing in this respect (Table 1). Stelling[118] also observed strong red shifts in the chloro complexes of Cr^{III} and Co^{II} such that the oxidation number of chlorine would have been more negative than −1. (This is readily explained in the molecular orbital (MO) theory, where the energy of the acceptor orbital may be expected to vary, the partly filled shells of chromium and cobalt probably playing the role of a low, accessible orbital[50].)

Collet[26] has studied the L_{III} edges ($2p \rightarrow 5d$ transition) in complexes involving Re^{IV}, Pt^{II} and Pt^{IV}. The relative shifts of the first acceptor orbital in the various Pt complexes agree (Table 2) fairly well with the spectroscopic result for transitions to the $d_{x^2-y^2}$ orbital in Pt^{II}, γ_3 in Pt^{IV}, assuming constant energies or a parallel development of $2p$ and

TABLE 1

K-edge shifts in some complexes involving 3*d* block metals

Metal and its oxidation state	Complex	Edge-shift (eV)	Ref.
Mn^{VII}	$KMnO_4$	20	89
Mn^{II}	$K_4Mn(CN)_6 \cdot 3H_2O$	13	89
Fe^{II}	$K_4Fe(CN)_6$	13	89
	$FeSO_4 \cdot 7H_2O$	5	89
Fe^{III}	$K_3Fe(CN)_6$	14 (soln.) 13 (solid)	89
Co^{II}	$CoCl_2 \cdot 6H_2O$	8	89
Co^{III}	$Co(en)_3(ClO_4)_3$	9	89
	$K_3Co(CN)_6$	10	89
Co^{II}	$Co(NO_3)_2 \cdot 6H_2O$	9.6	65
	Co–TMA (freshly prepared)	12.0	65
Co^{III}	Co–TMA (kept overnight in air)	16.4	65
	$Co(NH_3)_6Cl_3$	17.3	65
	$Na_3Co(NO_2)_6$	15.9	65
Co^{II}	$CoSO_4 \cdot 7H_2O$	8.7	85
	Co–TPA	7.7	85
Co^{III}	Co–TV	12.1	85
Cu^{I} ($Z_{eff} = 3.7$)	Cu–TV	0.7	85
Cu^{II} ($Z_{eff} = 4.55$)	$CuSO_4 \cdot 5H_2O$	6.5	85
	Cu–TPA	7.0	85
	Cu–TSA	5.1	85
	Cu–EA3CS	5.4	85
Cu^{III} ($Z_{eff} = 5.4$)	Cu–tellurate	15.6	85
Co^{II}	Co–bis-*S*-ethyl-1-amidino-2-thiourea	11 ± 1	2
Co^{III}	Co–isonitroso-acetyl-acetonate	15 ± 1	2

TABLE 2

X-ray absorption bands[26] in the group L_{III} ($2p_{3/2} \rightarrow 5d$)

Metal ion	Complex ion	X-ray band shift (in kK)	Optical transitions[a]
Pt^{II}	$Pt(CN)_4^{2-}$	71 ± 2	(35.7)[b]
	$Pt(SO_3)_4^{6-}$	68 ± 8	(40)
	$Pt(NH_2OH)_4^{2+}$	49 ± 2	(42)
	$Pt(SCN)_4^{2-}$	70 ± 7	(24) (37.4)
	$PtCl_4^{2-}$	34 ± 5	25.7
Pt^{IV}	$Pt(OH)_6^{2-}$	53 ± 5	(32)
	$PtCl_6^{2-}$	46 ± 7	28.3

[a] Wave number in kK of the first spin-allowed internal *d* shell transition.
[b] Values in parentheses estimated from spectrochemical series.

the filled *5d* sub-shell. L_{III} edge shifts of Pt and Au in some cyano and chloro complexes have also been measured by Nigam[78]. The present authors[85,114] have shown that the *K* edge shifts in the case of a number of complexes involving Cu^{I}, Cu^{II} and Cu^{III} and also Co^{II} and Co^{III} conform well with the valency dependence (Table 1).

(ii) Shift in the position of the principal absorption maximum

Valency change has also been inferred from the shift in the position of the main peak. Vainshtein et al.[123] observed that an increase in the valency of manganese in the order $MnO \rightarrow Mn_2O_3 \rightarrow MnO_2$ resulted in a systematic shift of the principal absorption maximum towards higher energy (Fig. 8) in agreement with Coster and Kiestra[31]. The effect is also exhibited[38] (Table 3) by the oxides and the acetyl acetonates of Mn, Fe and Co and has been related to the shift in the position of antibonding orbitals. However, their results[38] for ferro- and ferricyanides (like those whose main edge shift is discussed in Sect. C(i)) show an insignificant difference in energy. This appears to be consistent with Van Nordstrand's view[130] that "the nominal valency of the absorbing atom has an influence on the *K* edge fine structure of transition metals in some cases (e.g. MnO_4^-, MnO_4^{2-}, Mn–acetyl acetonates) while it has no influence in others (e.g. hexacyanides of Fe)". In the authors' investigations[81], the main peak for Cu^{I}–Thiovanol (TV) complex appears at an appreciably longer wavelength than those due to Cu^{II} complexes (Fig. 4).

(iii) Relation to effective nuclear and peripheral charges

Indirect evidence for valency change has been adduced from the determination[125] of the effective charge on the periphery of atoms in molecules by Barinskii[7,9]. Thus the effective charge of chromium, as calculated from the *K* edge fine structure, is found to be 0.2 for Cr^{6+}, 1.2 for Cr^{3+} and 1.9 for Cr^{2+} (and similarly for Mn and Co). The experimental data of Ovsyannikova et al.[94] and of Barinskii and Nadzhakov[10] clearly show that there exists a direct relationship between *K* and L_{III} edge shifts and effective coordination charge of the atoms in compounds. However, where there is no change either in the coordination or in the degree of ionicity of the bonds, the determining factor may be valency.

Becker[15] has shown that the nuclear charge number is related to the energy of the *K*-absorption edge. Very recently, the present authors[114] have also shown that the variation in the *K* edge shifts of copper in some complexes involving Cu^{I}, Cu^{II} and Cu^{III} follows a parallel variation in the calculated Z_{eff} (for the 4*p* shell), in agreement with Karalnik's explanation[51] of edge shifts based on external screening effects.

(iv) Investigations on mixed valency

Quite recently, Vishnoi[134] has shown that the L_{III} edge shift of lead in Pb_3O_4 is intermediate between those of PbO and PbO_2. Vainshtein et al.[123] have observed that the *K*-absorption spectrum of manganese in Mn_3O_4 (containing Mn^{II} and Mn^{III} in the ratio 1 : 2) practically coincides with that expected from an additive superposition of the

TABLE 3

Shift of the main peak as a function of oxidation state

Compound	Oxidation state	Main peak (eV above metal edge)	Ref.
$Mn(C_5H_7O_2)_2 \cdot 2H_2O$	+2	15.5	38
$Mn(C_5H_7O_2)_3$	+3	28.7	38
$Co(C_5H_7O_2)_2 \cdot 2H_2O$	+2	16.2	38
$Co(C_5H_7O_2)_3$	+3	26.4	38
$FeSO_4 \cdot 7H_2O$	+2	15.7	38
$Fe_2(SO_4)_3$	+3	23.3	38
Cu–TV	+1	11.4	81
Cu–TPA	+2	16.1	81
$CuSO_4 \cdot 5H_2O$	+2	14.1	81
Cu–TSA	+2	18.6	81
Cu–tellurate	+3	22.9	81

absorption edges of MnO and Mn_2O_3 in the ratio 1:2 (Fig. 8). These results indicate the possibility of gaining evidence for mixed valency from X-ray absorption spectra. This has recently been demonstrated[84] in the case of Cu^{I} and Cu^{II}, known to be involved together in copper–thiomalic acid[86] and copper–thiovanol[98] complexes. Two distinct edges were observed (Fig. 9) separated by ~10 eV, in agreement with the observations of Beaman et al.[13].

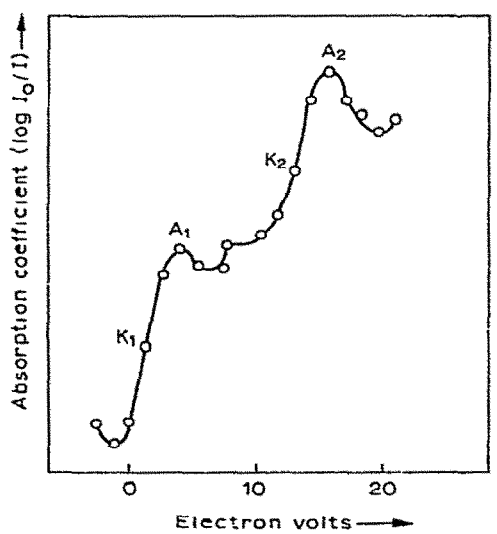

Fig. 9. *K*-absorption edge of copper in $Cu^{I,II}$–thiomalic acid complex.

TABLE 4

Edge-widths of some cobalt spinels (Keeling[53])

Absorber	Coordination symmetry	Edge-width (eV)
CoO	Octahedral	5.3
$Fe^{3+}[Co^{2+}Fe^{3+}]O_4$	Octahedral	6.8
$Ge[Co_2]O_4$	Octahedral	7.1
$Co[Al_2]O_4$	Tetrahedral	8.9
$Co[Cr_2]O_4$	Tetrahedral	9.0
$Co[Mn_2]O_4$	Tetrahedral	9.7

D. EDGE WIDTH AND COORDINATION STOICHIOMETRY

The energy difference between the inflection point of the absorption edge K and the principal absorption maximum A (Fig. 10) has been termed[53] the "edge width" (sometimes half edge width[14,24]). Keeling[53] has shown, from a measurement of K edge widths of cobalt in a number of cobalt spinels having well known nearest-neighbour arrangements that the edge width is significantly greater for compounds containing the metal ion in tetrahedral sites than for those in octahedral ones. The coordination symmetry of Co^{II} in $Co[Al_2]O_4$, whose observed magnetic moment (4.94 B.M.) is inconclusive in this respect, has been decided on this basis (Table 4). Very recently edge width measurements[83] on a number of cobalt, copper and lead complexes have led to an empirical correlation between edge width and coordination stoichiometry expressed in terms of the overall metal–nearest-neighbour electronegativity difference. The curve obtained between these two

Fig. 10. Microphotometer record of K-absorption edge of copper in Cu–TPA complex.

TABLE 5

Compound	Coordination stoichiometry	$\Sigma(X_M \sim X_L)$	λ_K (x.u.) ±0.05	λ_A (x.u.) ±0.05	Edge width (eV)	$[EW.\Sigma(\Delta X)]^{1/2}$	Ref.
	M:S:O						
$CuSO_4 \cdot 5H_2O$	1:–:6	9.6	1376.33	1375.19	7.6	8.5	83
Cu–TPA	1:2:4	7.6	1376.40	1374.87	9.1	8.3	83
Cu–TV	1:3:3[a]	6.6	1377.21	1375.57	10.7	8.4	83
Cu–TSA	1:4:2	5.6	1376.54	1374.50	13.5	8.7	83
Cu–EA3CS	1:1:3	5.4	1376.47	1374.38	13.7	8.7	83
Pb–TPA	1:1:3	5.8	947.75	947.83	12.6	8.5	83
Pb–TSA	1:1:3	5.8	948.56	947.46	13.9	9.0	83
	M:O[b]						
Cu–oxal	1:6	9.6	1376.2	1375.08	7.5	8.4	112, 115
Cu–acet	1:5	8.0	1375.29	1374.01	8.4	8.2	112, 115
Cu–tellur	1:6[b]	9.6	1375.26	1374.17	7.2	8.3	112, 115
	Co:S:O						
$CoSO_4.7H_2O$	1:–:6	10.2	1601.96	1600.91	5.0	7.1	85
Co–TPA	1:2:4	8.2	1602.48	1600.85	6.8	7.4	85
Co–TV	1:3:3	7.2	1601.19	1599.55	7.2	7.2	85
	Co:O						
CoO	1:6	10.2			5.3	7.3	53
$Co[Al_2]O_4$	1:4	6.8			8.9	7.8	53
$Co[Cr_2]O_4$	1:4	6.8			9.0	7.8	53
	Zr:O						
ZrO_2	1:7	14.7			17.8	16.2	36
$ZrSO_4.4H_2O$	1:8	16.8			16.0	16.4	36
$ZrOCl_2$	1:8	16.8			16.5	16.6	36
	Nb:O:F						
K_2NbOF_5	1:1:5	13.9			28.0	19.7	79
$(NH_4)_2NbOF_5$	1:1:5	13.9			28.0	19.7	79
K_3NbOF_6	1:1:6	16.3			23.0	19.3	79

[a] Estimated from edge width measurements.
[b] M = Cu, Pb.

quantities resembles a rectangular hyperbola (Fig. 11) and may be represented (for a given metal in a given region) by the equation

$$[\Sigma(X_M \sim X_L) \cdot \text{edge width}]^{1/2} = \text{constant}$$

where X_M and X_L are the Pauling electronegativities of the central metal atom and the nearest neighbours respectively. The relationship has been verified[112] using data that have appeared in the literature (Table 5)[36,52,79]. The average values of the constants for cobalt

and copper, both of the first transition series, are respectively 7.7 and 8.5, while those for zirconium and niobium, both of the second transition series, are respectively 16.4 and 19.1. It may be noted that edge width and $\Sigma(X_M \sim X_L)$ may be taken roughly to define band width and the ionic/covalent character of the M–L bond respectively. The band width may be expected to increase with an increase in the degree of covalency of the bond, which, in turn, is known to follow a decrease in the value of $(X_M \sim X_L)$. The relationship mentioned above thus seems to be valid.

E. STRUCTURE OF THE ABSORPTION EDGE AND COORDINATION SYMMETRY

The variations in intensity in the different regions of the absorption edge, which gives rise to a characteristic shape of the absorption coefficient curve, have been correlated (refs. 38, 128, 129) with many stereochemical features of a coordination complex. The X-ray intensity is given by the product of transition probability and the density of states, and the latter depends upon the number, nature and symmetry of the nearest neighbours[11,30,43]. Thus according to Jørgensen[50], in an octahedral complex the only possible Laporte-allowed and symmetry-allowed transitions are from γ_1 (1*s*) to the odd ν_4 (4*p*) orbitals and the various empty molecular orbitals will show up in absorption, in accordance with the amount of *p*-behaviour close to the nucleus of the central metal atom. Glen and Dod[38] and, more recently, Seka and Hanson[108] have systematically developed the application of

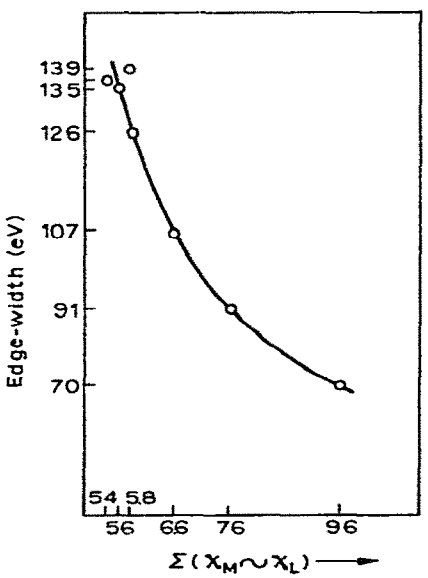

Fig. 11. Variation of $\Sigma(X_M \sim X_L)$ with edge width of copper (and lead) in some complexes.

MO theory to interpret the main features of the structure of the *K*-absorption edge for a good number of coordination complexes involving first transition series metal ions. It is now known[12,42] that the structure of the X-ray absorption edge is decided to a large extent by the nature of the immediate surroundings of the atom or ion in question. Kauer[52], Boke[22], Collet[26] and Mande and Chetal[62,63,65] have shown that the inferences drawn from edge-structure studies are compatible with magnetic measurements.

The features most relevant to the study of the stereochemistry of a complex are:

(*a*) The shape of the edge;

(*b*) Structures appearing to the long-wave side of the principal absorption maximum, and

(*c*) Splitting or broadening of the main peak.

(i) Shape of the edge

Van Nordstrand[128,129] has recently classified the *K*-absorption curves of a variety of solids involving transition metals into four categories, as shown in Table 6 and Fig. 1.

TABLE 6

Type	Examples	Structural features
I_A ($MnCl_2.4H_2O$)	Hydrates, and Mn, Co, Ni etc. salts and solutions	Octahedral coordination by oxygen
I_B	Complexes of trivalent Cr, Mn, Co, etc.	Octahedral coordination by NH_3, en, NO_2^-, CH_3COO^- etc.
II ($K_3Mn(CN)_6$)	$K_3Co(CN)_6$ (crystals and soln.), $K_3Cr(CN)_6$, $Cr(CO)_6$	Octahedral coordination by linear ligands, e.g. CN^-, CO
III (Mn metal)	Metals and metallic phases; carbides, sulphides, bromides etc.	(electronic conduction, polarizability etc.)
IV_A	MnO_4^-, CrO_4^{2-}, CrO_7^{2-}	Tetrahedral coordination; central atom with formal valency corresponding to argon core
IV_B	MnO_4^-	Tetrahedral coordination

The principal features of these spectra have been explained by Sinha and Mande[110] on the basis of ligand field theory. Mande and Chetal[62,63,65] and Padalia and Krishnan[96] have determined the symmetry occurring in a series of cobalt complexes by reference to this classification. However, the characterization is limited to perfectly octahedral and tetrahedral coordination symmetries.

(ii) Low-energy absorption and coordination symmetry

Gusatinskii and Ischenko[39] have shown that the initial region of the absorption

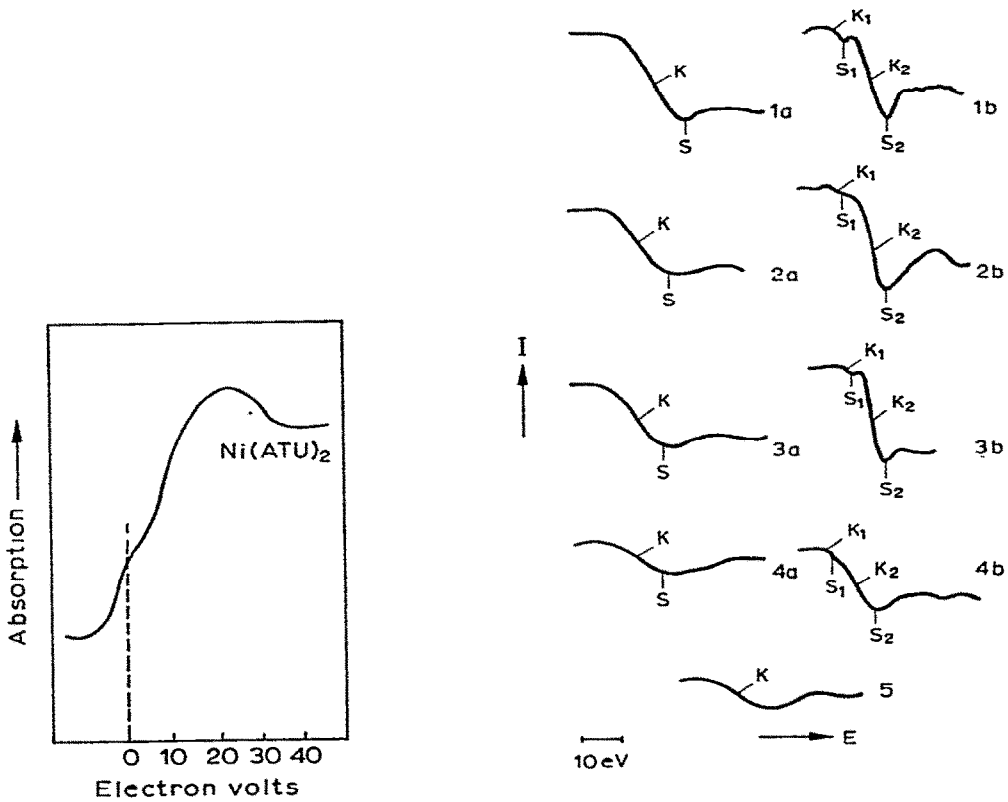

Fig. 12. *K*-absorption edge of nickel in Ni–$(ATU)_2$.

Fig. 13. *K*-absorption edges of cobalt in pink and blue cobalt chloride solutions (1a, 1b); hydrated and anhydrous cobalt oxinates (2a, 2b); α- and β-bis-(pyridine) cobalt chlorides (3a, 3b); diquinolinium cobalt chlorides (pink solution and blue solid) (4a, 4b); cobalt–TMA complex (5).

spectrum (i.e. the long-wave feature) depends upon the character of the first coordination polyhedron of the absorbing atom. In the *K*-spectra of the first transition series Albrecht[3] and Glen and Dod[38] have shown that the relaxation of selection rules for the $1s \rightarrow 3d$ quadrupole transition in the *K*-absorption region occurs in asymmetrically coordinated metal atoms, especially those with one or zero $3d$ electrons. According to Mitchell and Beaman[72] the expectation of this absorption for planar and tetrahedral symmetry involving sd^3 bonding in some covalent complexes of Cr, Mn, Fe and Ni has been confirmed by experiments[42,72,104,135]. The planar $Ni(CN)_4^{2-}$ complex exhibits[37,72,73,92,124] a pronounced low-energy absorption in the $3d$ region. Very recently, Padalia and Gupta[95] have investigated the *K*-absorption spectrum of Ni^{II}–1-amidino-2-thiourea (Ni^{II}–ATU) and have thereby proposed a planar configuration in agreement with earlier findings[97] (Fig. 12). Van Nordstrand's classification, distinguishing type IV spectra characteristic of

tetrahedral coordination, is based upon the criterion of low-energy absorption. Mande and Chetal[62,63] have determined the coordination number and symmetry in the hydrated and anhydrous oxinate complexes of cobalt (Fig. 13) and also in the pink and blue cobalt chloride solutions (Fig. 13) on this basis. Padalia and Krishnan[96] have also observed that the *K*-absorption edge of cobalt in the tetrahedral complex diphenyldithiophosphinate—Co^{II} ($Co[DPDTP]_2$) shows a splitting whereas tris(isonitrosacetato-phenonato)Co^{III} ($Co[INAP]_3$) gives rise to a monotonic curve supporting its octahedral coordination symmetry. Similar observations have been made by the present authors[111] in the case of some mercury and uranium complexes[70,71,87] which have been shown to be respectively 4- and 6-coordinated (Figs. 22,23). However, inasmuch as low-lying absorption has been attributed to tetrahedral coordination, there are many deviations from it. Thus, Ni^{II}—bis-salicylaldehyde dihydrate, studied earlier by Mitchell and Beaman[72], shows such a low-lying maximum (usually described[43] as being due to a $1s \rightarrow 3d$ transition) but has been suggested by Cotton and Hanson[35] to be octahedral.

(iii) Modulations of the principal absorption maximum

In general, ionic salts give sharply peaked *K*-absorption edges, while in covalent compounds some broadening is observed. A broadening or splitting of the *K*-absorption maximum is also an indication of a splitting of the degenerate energy levels of the atom, which in turn is an indication of unsymmetrical metal-to-ligand bonding[38] and/or of the spectroscopic splitting effect of the particular ligand. A quantum-mechanical analysis of the symmetry dependence of the crystal field splitting of *p*-orbital degeneracy by Cotton and Ballhausen[32] has shown that the degenerate *p*-level, and hence the *K*-absorption maximum (of the first transition series element), remains unsplit in a regular octahedral

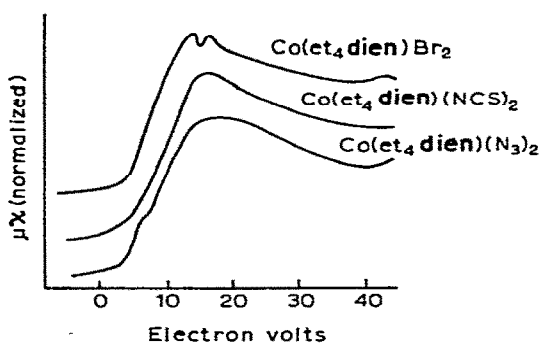

Fig. 14. Spectra of five-coordinate cobalt complexes.

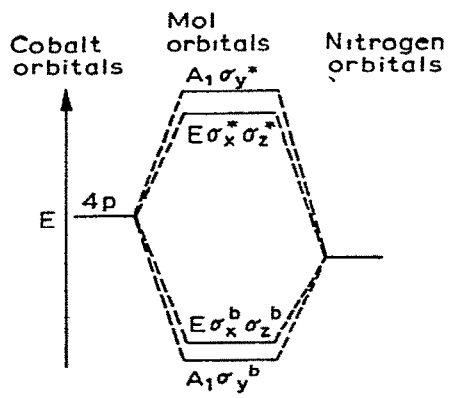

Fig. 15. Partial MO energy level diagram for C_{3v}.

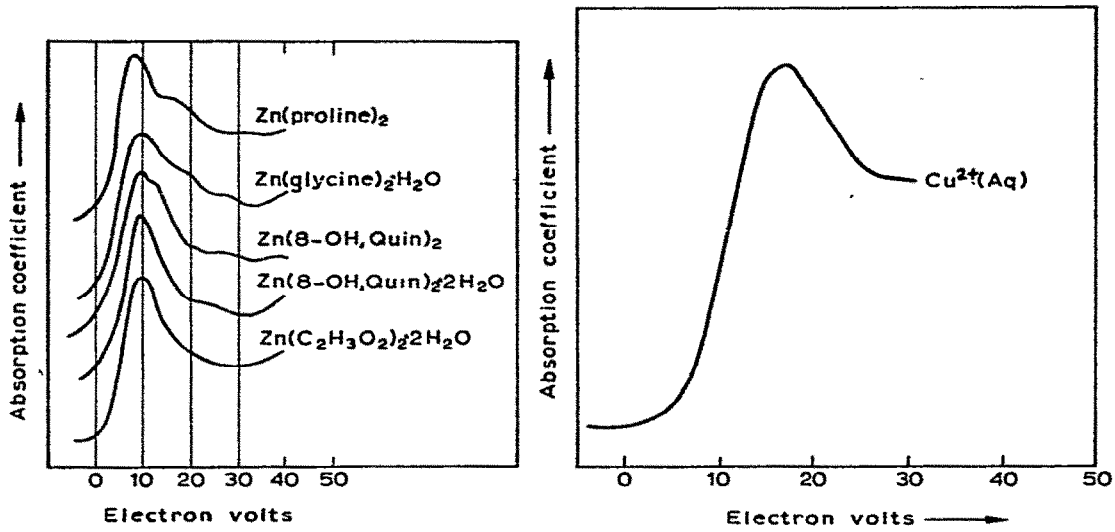

Fig. 16. *K*-absorption edges of Zn^{2+} ions in ligand fields of lower than average octahedral symmetry.

Fig. 17. *K*-absorption edge of Cu^{2+}(aq.).

(O_h) field while it splits up into two or more components as the coordination symmetry is lowered (for example in D_{4h}, $\Gamma_p = A_{2u} + E_u$). This has been verified by Cotton and Hanson[33,34], for instance, with some copper and zinc complexes, by the appearance of a double *K*-absorption peak for $Cu(NH_3)_4^{2+}$ (aq.) (D_{4h}) (Fig. 5). Glen and Dod[38] have observed that the principal absorption maximum of cobalt in $Co(et_4dien)(N_3)_2$ and $Co(et_4dien)_2(NCS)_2$ remains broadened only while it is split up into two components in the case of $Co(et_4dien)Br_2$ (Fig. 14). This is in agreement with the respective MO energy level considerations as illustrated in Fig. 15.

Where the splitting due to asymmetry tends to be smaller than can be resolved in the X-ray region, the spectra are characterized by generally broadened peaks, as observed, for example, in the case of Cu^{II} and Zn^{II} DL-prolinate dihydrate[33,34] (Figs. 9, 16). In the case of Cu^{II}–thiopropionic acid (D_{2h}) and Cu^{II}–thiosalicylic acid (D_{4h}) complexes, the main peak[81] due to the former is apparently split up into two rather broad maxima (three would be expected[32]) whereas the latter shows only a single broad peak (two expected[32]) (Fig. 4). Similarly the *K*-absorption maximum in the case of the cobalt–thiovanol complex (Fig. 3) is also seen to split up into two components (symmetry[85] C_{2v}). (Vainshtein et al.[126] observed *d*-orbital splitting in the case of TiO_2 and TiC in the low energy ($3d$) region of the *K*-absorption edge of the metal (Fig. 2).)

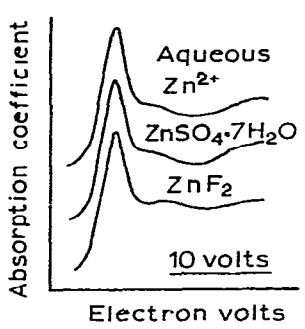

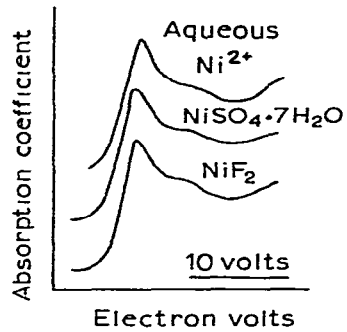

Fig. 18. Ni *K*-absorption edges (octahedral symmetry).

Fig. 19. Zn *K*-absorption edges (octahedral symmetry).

F. INFLUENCE OF THE NATURE OF LIGANDS

(i) Spectra of aquated complexes

The aquated ions, particularly[14,33,34,41] of Cr to Zn, give simple edge structures (Figs. 17, 18, 19) with the main peaks unsplit and a second broad maximum ($1s \rightarrow 5p$) appearing on the short-wave side. In many cases, the structure and energy of the *K*-edge of a complex is practically identical in the solid and in solution[42,43]. Thus Ni^{2+} in solution and in the hydrated salt have essentially identical structures[41] (Fig. 18). Beaman and Bearden[14] have shown that the Cu^{2+} ion in aqueous solution absorbs as if in vacuum and that the structure is due to the excitation of the *K* electron into the optical levels of the ion[24]. They have devised a cycle for calculating *K* edge shifts from optical data. According to Hanson[41], a calculation of the radial distribution of the $4p$ state associated with *K*-excitation shows the maximum radial probability to be as large as the distance of the hydration layer from the central ion. The overall splitting of the ground state of the ions having unfilled $3d$ and $4p$ orbitals due to the cubic perturbing field of the hexa-aquated ions[101] may be the cause of some broadening of the main peak of the *K* edge, observed by Beaman and Bearden[14] in the case of aqueous solutions of Ni^{2+}, Cu^{2+} and Zn^{2+}. The fact that Zn^{2+} has a filled $3d$ shell probably explains a narrower $1s \rightarrow 4p$ absorption line for Zn^{2+} (edge-peak separation $\Delta = 8.7$ eV) than for Cu^{2+} ($\Delta = 16.7$ eV) and Ni^{2+} ($\Delta = 17.9$ eV). This may be compared with the energies of the absorption bands in the optical region as shown in Table 7.

Mande and Chetal[62] have solved the problem of the pink and blue cobalt chloride solutions – both involving Co^{2+} (aq.) – on the basis of Van Nordstrand's classification (refs. 128, 129) of edge shapes, and have shown that the cobalt ion in the two is aquated in octahedral and tetrahedral symmetries respectively (Fig. 13), in agreement with optical[48] and

TABLE 7

$Ni(H_2O)_6^{2+}$	9,000 cm^{-1} (1.1 eV)	$^3A_{2g} \rightarrow {}^3T_{2g}$
	14,000 cm^{-1}	$^3A_{2g} \rightarrow {}^3T_{1g}$ (F)
	25,000 cm^{-1}	$^3A_{2g} \rightarrow {}^3T_{1g}$ (P)
$Cu(H_2O)_6^{2+}$	12,600 cm^{-1} (~1.5 eV)	

crystallographic[49,74,75,102] studies. The fine structure of K-absorption spectra of Ni^{2+}, Cu^{2+} and Zn^{2+} etc. have been investigated by Cauchois[24] and others[124]. The distant absorption bands have been attributed[24] to the interaction of the X-ray photoelectron with the edifice of water molecules in agreement with the results of Raman and optical spectra of ionic solutions.

(ii) Spectra of nitrogen ligand complexes

According to Kauer[52], the ammonia ligand is unique in causing splitting of the K-absorption maximum of first transition series metals irrespective of symmetry considerations. Thus $Cu(NH_3)_4^{2+}$(aq.) (D_{4h}) shows[14,33] a double maximum (ΔE=~5 eV) (Fig. 5), in agreement with Cotton and Ballhausen[32]. $Co(NH_3)_6^{2+}$, $Ni(NH_3)_6^{2+}$, and $Ni(en)_3^{2+}$ (all O_h) also show[35,52] this effect (ΔE=~25 kK, i.e. ~3 eV), suggesting that in these cases two MO energy levels occur with this energy separation (~3 eV)[50]. $Zn(NH_3)_4^{2+}$ (aq.) shows a splitting of about 10 eV while $Zn(en)_3SO_4$ does not[35] (Fig. 20), and nor do α- and β-bis-pyridine Co^{II} chlorides[65] (Fig. 13). The splitting, however, appears faintly[89] in the case of $Co(en)_3(ClO_4)_3$ and $Co(NH_3)_6Cl_3$. It is of interest to note that in the ammonia complexes, while the energy for internal d-shell transition (c.f.s.e.) ranges from 1–3 eV (10–30 kK), that observed for p-orbital splitting ranges from ~3–10 eV, as illustrated in Table 8.

TABLE 8

Complex	c.f.s.e.	Splitting of the main peak ($1s \rightarrow 4p$)	Ref.
$Cu(NH_3)_4(H_2O)_2^{2+}$	17 kK (2.1 eV)	5 eV	33
$Co(NH_3)_6^{2+}$	23 kK (2.8 eV)	11 eV	89

(iii) Spectra of sulphur ligand complexes

As discussed earlier (Sect. E (iii)), the symmetry dependence of the p-orbital splitting does not satisfactorily explain the observation that in the case of the complexes $[Cu(NH_3)_4(H_2O)_2]^{2+}$ and $[Cu(TSA)_4(H_2O)_2]^{2-}$, which have the same symmetry (D_{4h}),

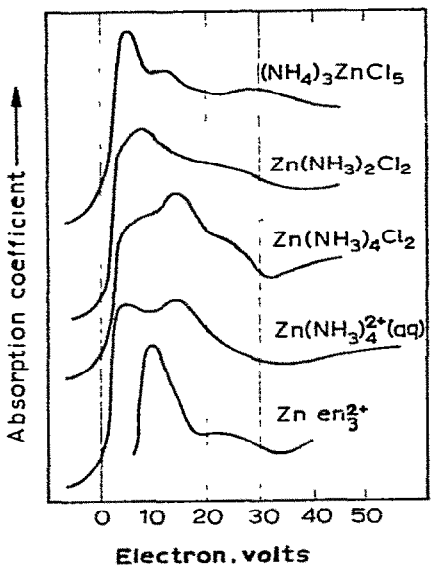

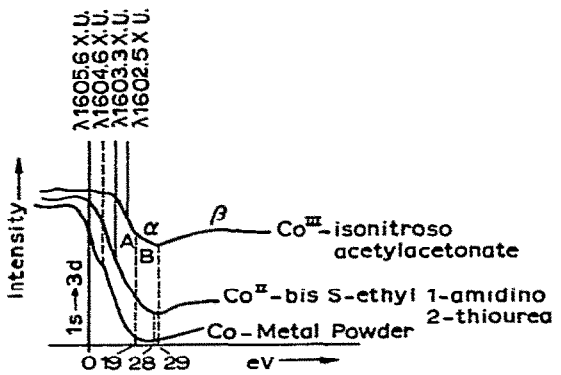

Fig. 20. *K*-absorption edges of zinc ions in ligand fields of known or presumed tetrahedral symmetries.

Fig. 21. Microphotometer records of the Co *K* edge in the metal and two chelates.

the former shows a splitting of the *K*-absorption maximum whereas the latter shows only a broadening. This may be due to a smaller spectroscopic splitting effect, as suggested by the position of sulphur ligands in the spectrochemical series. Sulphur ligands have usually been found to cause a broadening of the *K*-absorption maximum, as observed by Padalia and Gupta[95] for Ni^{II}–ATU (Fig. 12), by Agarwal and Nigam[2] (Fig. 21), and the present authors and Pandey[81,111] (Figs. 4, 22). Cu^{II}–TPA has been shown to involve Jahn–Teller distortion, a broad band appearing at 15,600 cm^{-1} ($2E_g \rightarrow 2T_{2g}$). It is of interest to compare the energy (c.f.s.e.) of this band (~1.9 eV) and the observed *p*-orbital (*K*-absorption maximum) splitting[81] of ~5 eV with the corresponding data for $[Cu(NH_3)_4(H_2O)_2]^{2+}$ described earlier (Table 8).

The features of edge structure generally observed for the *K*-absorption edges of complexes of metals of the first transition series may be broadly compared with the qualitative MO energy-level diagram of an octahedral complex as shown in Fig. 2(b).

(iv) The spectrochemical effect

While the spectrochemical and nephelauxetic series have hitherto been determined on the basis of the spectroscopic splitting parameter and 10 *Dq* values in the optical region, Seka and Hanson[108] and the present authors[81,117] have recently attempted to show that such a correlation could possibly be made on the basis of X-ray absorption spectra as well.

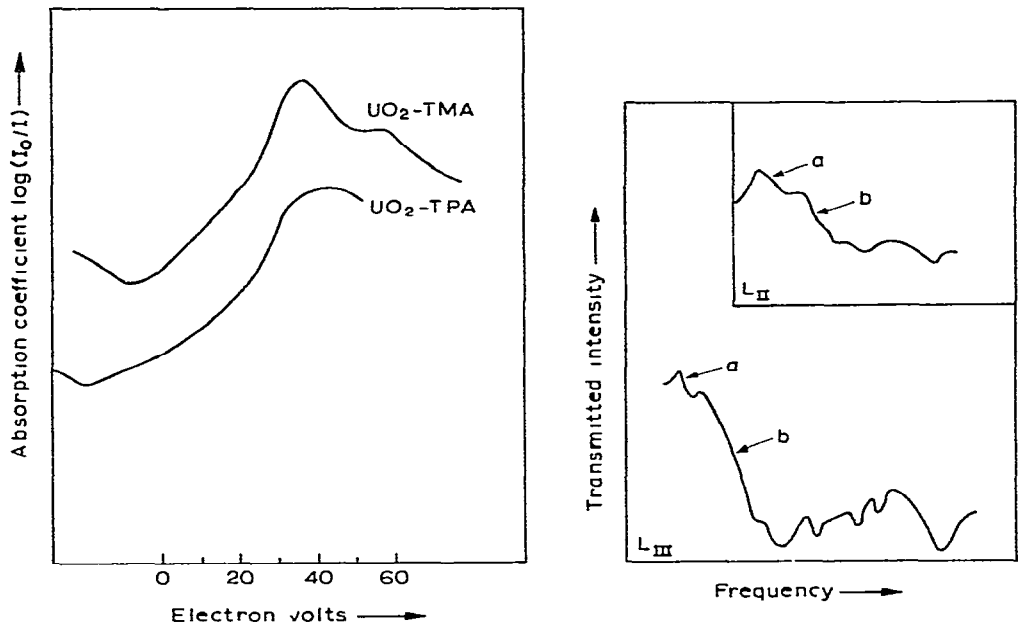

Fig. 22. L_{III} absorption edge of uranium in some complexes.

Fig. 23. L_{II} and L_{III} absorption edges of mercury in Hg^{II}–TPA.

Seka and Hanson have found that the $a_{1g}^* - t_{1u}^*$ level separation observed on the K edge of iron in some octahedral complexes is related to the spectrochemical series in the same way as the optical $t_{2g} - e_g^*$ separation. The present authors have observed that whereas $Cu(NH_3)_4(NO_3)_2$ and $Cu(py)_4SO_4$ give rise to sharp splittings[33] of the main peak, $Cu^{II}(TSA)_4(H_2O)_2$, which has a similar coordination symmetry[76] but has sulphur donors in place of nitrogen, does not show this splitting but shows only a general broadening. It has been argued that sulphur donor groups, which are much lower than NH_3 or pyridine in the spectrochemical series[93], are probably unable to cause a large enough splitting to be discernible by the relatively poor resolution of X-ray work[33]. The splitting of the main peak[38] on replacing N_3 or NCS by Br in $Co(et_4dien)X_2$ ($X = N_3$, NCS, Br) may be due either to the lower electronegativity of Br relative to N or to lowering of symmetry, or both; the other two complexes show only extensive broadening (Fig. 14).

G. NATURE OF THE METAL–LIGAND BOND

(i) Edge structure and homopolar bonding

The K-absorption edges of first transition series elements have been studied from this

standpoint by a number of investigators[42,43,72,88-92,104,121,122]. In general, ionic solids give rise to sharply peaked edges, whereas in covalent compounds these are somewhat broadened[41]. Thus the present authors[85] have observed that the $1s \rightarrow 4p$ absorption for cobalt in $CoSO_4.7H_2O$ is sharp, while it is broadened (or split) in the complexes Co–TPA and Co–TV, which have been shown to be appreciably covalent[69,99] (Fig. 3). As suggested earlier, the low-energy absorption too has some bearing on the nature of bonding. Thus according to Hanson and Beaman[42] the amount of absorption in the $3d$ range increases with the amount of electron sharing. From the study of a series of ionic compounds of the first row transition metals, Hanson and Knight[43] have observed that this absorption is most prominent in the case where the binding is least ionic and the symmetry lowest. Vainshtein[124] has shown that the K edge of Ni^{2+} in the aqueous and alcoholic solutions of its chloride and sulphate is characterized by the absence of distortion on the long-wave side whereas this is clearly observed in the covalent $Ni(CN)_4^{2-}$ (aq.) ion. In the K-absorption spectra of some copper complexes[81], faint long-wave maxima in Cu^{II}–thiopropionic acid and Cu^{II}–thiosalicylic acid complexes have been observed (Fig. 4); the complexes have been shown to be appreciably covalent[68,76] on the basis of their spectral and magnetic properties. Similarly in the cobalt complexes the low energy absorption is seen to be quite pronounced (Fig. 3).

(ii) Relation to edge shifts and edge widths

Quite recently Agarwal and Verma[1] have suggested that for metal ion species in the same oxidation states, the edge shift is suppressed with an increase in the degree of covalency of the compound. The observations have been supported by the results of Srivastava et al.[113,114] on the K edge shift of copper and L_{III} edge shift of lead in some complexes. The ligand thiosalicylic acid has on this basis, as also on the basis of some IR spectral measurements[113], been shown to impart a greater degree of covalency to the metal–sulphur bond than thiopropionic acid. A similar conclusion has been drawn on the basis of edge width measurements on these complexes[83]; edge widths have been observed to increase with increase of covalent character. This is also suggested by the empirical relationship mentioned earlier (p. 286).

(iii) Spectral shifts and the nephelauxetic effect

Glen and Dod[38] have observed a high-energy shift of the K-absorption maximum of cobalt in Co $(et_4dien)X_2$ ($et_4dien = HN[CH_2CH_2N(C_2H_5)_2]_2$; X = Br, NCS and N_3) in the order $N_3 \rightarrow NCS \rightarrow Br$, and have related this to the increase in covalent bond strength of the Co–X bond in the same order. In the series $YCl_3 \rightarrow Y(NO_3)_3 \rightarrow Y_2(SO_4)_3$, in which the magnetic susceptibility decreases in the same order, Bhide[18] has observed that the K-absorption maximum of yttrium shows a parallel shift to the lower frequency side (Fig. 7), indicating the lowering of $5p$ levels due to homopolar bonding. Beaman and

Bearden[14] have shown that the energy of the K-absorption maximum of copper in $Cu(H_2O)_6^{2+}$, $Cu(NH_3)_4^{2+}$ and $Cu_2(CN)_4^{2-}$ increases in this order. These effects are indeed manifestations of the influence of the nature of the central ion or of the ligands on the metal–ligand bond. The position of a particular ligand in the nephelauxetic series is usually determined from the electronic absorption spectroscopic data. However, an attempt has recently been made[81] to show that the relative energies of the K-absorption maximum of the metal ion in different complexes may also be interpreted in a similar manner. The sequence thus assigned to the various ligands (Table 3) in some copper complexes has been shown to be

$$RS^- \rightarrow C_5H_5N \sim NH_3 \rightarrow H_2O$$

It is seen that this agrees satisfactorily with the nephelauxetic series.

H. THE FINE STRUCTURE

The fine structure, i.e. the fluctuations in intensity observed on the high-energy side of the X-ray absorption edge, have been extensively studied both experimentally and theoretically[19,23,40,44-47,54-60,64,109,120,130]. An excellent review dealing with the theoretical aspects has been published by Azaroff[5]. The early studies have shown that this fine structure depends on the chemical states of the atom under investigation[27] and empirical relationships were found between the two, particularly for the compounds of the first transition series elements[128]. Obashi and Nakamura[88] have observed that for some simple and complex compounds of copper having similar coordination symmetries, the K-absorption fine structures almost coincide. They have concluded that the fine structure is mainly determined by the immediate surroundings of the atom in question in a region up to about 100 eV from the main edge. Sawada et al.[106] have found no difference in the K edge fine structure spectra of Fe^{2+}, Ni^{2+}, Cu^{2+} and Zn^{2+} between α- and β- phthalocyanine complexes, this difference being expected from the influence of the crystal lattice according to the Kronig theory. Their observations support those of Coster[28]. Bhide and Bhat[19] have invoked the plasma oscillation theory to explain the K-absorption fine structure close to the main edge in the case of yttrium. Van Nordstrand[130] has drawn the following generalizations with regard to the K edge fine structure spectra of coordination complexes of the first transition series elements.

(1) Fine structure extends up to 100 eV above the edge.

(2) Fine structure is determined solely by the complex itself, not by its state in a crystal or a solution, nor by its neutralizing ions.

(3) Fine structure is determined solely by the ligands; the central absorbing atom merely determines the location of the edge.

(4) The nominal valence of the absorbing atom has an influence in some cases (e.g. MnO_4^- vs. MnO_4^{2-}; acetyl acetonates of manganese), but has no influence in other cases (e.g. CrO_4^{2-} vs. MnO_4^-; hexacyanides of iron).

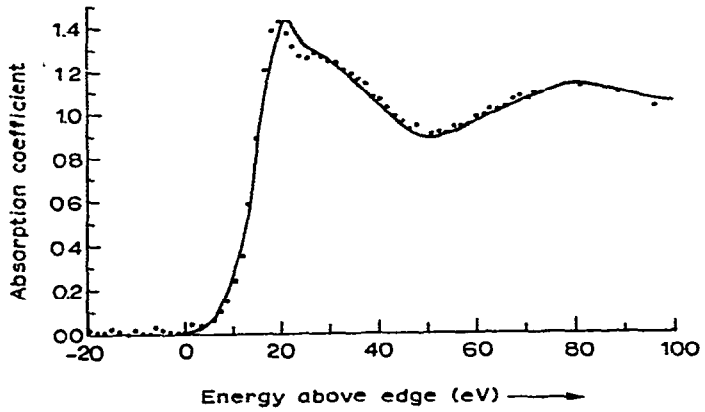

Fig. 24(a). *K*-absorption edge of chromium in $Cr(en)_2(NCS)_2$.

(5) In a mixed-ligand complex the fine structure spectrum is additively composed of the fine structure spectra of the corresponding unmixed-ligand complexes[107,131].

(i) Additivity of fine structure in mixed-ligand complexes

The first compounds to be studied in this connection were the bridged carbonyls of cobalt[132]. The spectrum of the simple carbonyl ligand (from the spectrum of chromium hexacarbonyl) may be subtracted from that of $Co_2(CO)_8$ to give the spectrum of bridging bonds, which may be imagined as

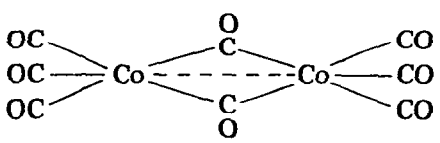

Earlier, Boke[22], from a study of some mixed-ligand complexes, stated that if a complex has two types of ligands the absorption spectrum will be intermediate between those characteristic of the two ligands. Recently, Van Nordstrand[130] has shown that the fine-structure spectrum of the mixed-ligand complex $[Cr(en)_2(NCS)_2]$ (the dotted curve in Fig. 24(a)) could be matched with the hypothetical blend (solid curve in Fig. 24(a)) of 4 moles $[Cr(en)_3]^{3+}$ and 2 moles $[Cr(NCS)_6]^{3-}$ (Fig. 24(b)). Similarly, Obashi[92] has observed that the fine structure due to $Ni(CN)_2.4H_2O$ closely resembles that due to an equimolecular mixture of $NiSO_4.6H_2O$ and $K_2Ni(CN)_4$. $Ni(CN_2).4H_2O$ is known to contain the square covalent complex $[Ni(CN)_4]^{2-}$ and the octahedral ionic complex $[Ni(H_2O)_6]^{2+}$ in equal proportion.

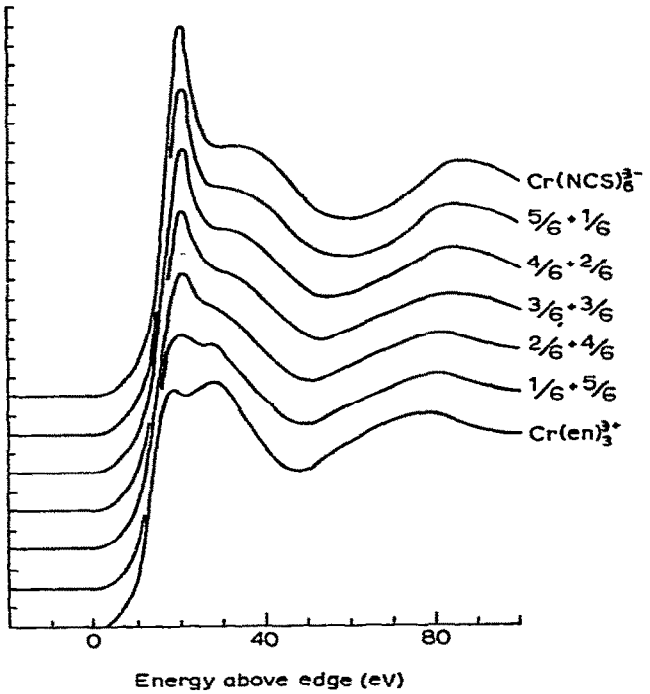

Fig. 24(b). Hypothetical blending of *K*-absorption curve for $Cr(NCS)_6^{3-}$ and $Cr(en)_3^{3+}$.

(ii) Determination of metal–ligand bond length

Hartree et al.[44] were the first to relate the intermediate fine structure (5–100 eV) in coordination complexes with their stereochemical aspects. According to them: (1) the amplitude of the fluctuations constituting the intermediate fine structure is proportional to the coordination number if the ligands are identical; (2) the energy values for the maxima and minima are determined by the radius of the coordination sphere; as the radius decreases all the features of the fine structure shift to the higher energy side. The metal–nearest neighbour bond distance (λr) was thus shown to be quantitatively related[13,44] to the energy (ΔE) of the first absorption maximum through the Bragg relation

$$\lambda r = \left(\frac{150}{\Delta E}\right)^{\frac{1}{2}}$$

According to Van Nordstrand[130], the fine structure is solely determined by the complex itself and not by its state in a crystal or by its neutralizing ions. Investigations on fine-structure spectra of coordination complexes have been carried out by other workers[89,105]. According to Levy[60], the absorption maximum at B (on the absorption coefficient curve)

corresponds to a transition from 1*s* to a vacant *p*-level and the maximum at C to a kind of ionization or escape energy of the 1*s* electron. Further, the difference in energy ΔE from the minimum at C to the maximum at D gives a measure of the radius of the coordination sphere around the central metal atom through the Bragg relation

$$r_1 = \left(\frac{151}{\Delta E}\right)^{1/2}$$

Mande[64] has utilized the method to determine the bond length in some cobalt compounds (Table 9) and the results are in good agreement with those from X-ray diffraction; the bond length in the cobalt–thiomalic acid complex[80,82] has been determined on this basis. These investigations were carried out in the solution state. However, the metal–ligand bond length in the complex $K_3Co(CN)_6$ (on the basis of the fine structure data obtained in the solid state by Obashi[89]) could also be computed[116] using the energy separation Δ(C~D) (Fig. 10). (The markings A, B, C ... here are somewhat different from those used in ref. 60.) The value of 1.85 Å obtained thus agrees well with that obtained from X-ray diffraction (1.89 Å). The results of similar fine structure measurements attempted on some copper compounds by the present authors[116] are given in Table 10. Bhide and Bhat[19] have used Lytle's analysis[61a] to determine the radius of the first coordination sphere of yttrium in the metal and its compounds and have compared the results with those obtained by using Levy's method and by X-ray diffraction. As Table 11 shows, it appears that Levy's method gives somewhat better agreement with the results of X-ray diffraction.

I. CONCLUSIONS – SOME UNSOLVED PROBLEMS AND FUTURE TRENDS

X-ray absorption spectroscopy thus offers an effective tool for investigating many vital problems of coordination chemistry such as valency of the metal ion, symmetry of the coordination sphere, nature of the metal–ligand bond, etc., when many other methods such as X-ray diffraction (particularly when the samples are solutions or are amorphous) and magnetic measurements (where the results are often ambiguous) fail to provide a full and satisfactory solution. However, the impact of this technique still

TABLE 9

Sample	Mande[64]	Levy[60]	X-ray diffraction
Co (metal)	2.5 ± 0.1	2.57 ± 0.15	2.50
$CoCO_3$	1.97 ± 0.1	1.98 ± 0.1	1.99
$CoSO_4.7H_2O$	1.98 ± 0.1	2.01 ± 0.1	1.99
Co^{III}–TMA	2.27 ± 0.1	2.01 ± 0.1	1.99

TABLE 10

Substance	Δ(C~D) (eV)	r (Å)	r (X-ray diffraction) (Å)
Cu (metal)	25	2.45	2.55
$CuSO_4.5H_2O$	38	1.99	2.0 (for Cu–O in sq. plane)
Cu–TPA	29	2.38	
Cu–TSA	31	2.20	

remains in its preliminary stage and requires thorough investigation, particularly on a quantitative basis. The *p*-orbital splitting requires a detailed study in relation to the energies of *d*-orbital splittings observed in optical spectra. The latter, amounting to about 2–3 eV in the case of first transition series metals, can be studied as such by X-ray absorption spectra[3,126]. Similarly, the mixed-valency effect should be tested further. The predictability of coordination stoichiometry from edge width data[83] requires some refinement in order to be more rigorous.

In the same way the method of bond length determination gives only the average radius of the coordination sphere, whereas individual metal–donor bond lengths could be computed from the data on the basis of charges on individual atoms in the coordination sphere. Investigations on "outer complexes" and complexes involving metal–metal interactions provide almost a virgin field. Spectroscopic characterizations, such as the edge shapes and the energies of edge features, particularly the frequencies of absorption maxima, need to be standardized. On the experimental side, as suggested by Hanson[41] and Jørgensen[50], the need for vacuum spectrographs of higher resolution and the use of very thin and perfectly uniform absorbing screens etc. should be greatly emphasized. Finally, it may be hoped that with the combined attack of determinations of the valency of the metal ion, the coordination symmetry and stoichiometry and the metal–ligand bond length, etc., the technique may be able to provide a complete perspective of the molecular structure of a coordination complex.

TABLE 11

Compound	Absorption – Levy's method (bond length) (Å)	Absorption – Lytle's method (unit sphere radius) (Å)	Diffraction interatomic distance (Å)
Yttrium oxide	2.11	2.35	2.27
Yttrium chloride	2.27	2.39	2.58
Yttrium hydroxide	2.54	2.61	2.54
Yttrium sulphate	3.43	3.33	3.28
Yttrium nitrate	3.30	3.58	
Yttrium metal	5.14	5.48	5.13

REFERENCES

1 Agarwal, B.K. and L.P. Verma, *J. Phys. C*, 3 (1970) 535.
2 Agarwal, R.M. and A.N. Nigam, *Proc. Indian Acad. Sci.*, 63 (1966) 200.
3 Albrecht, G., *Int. Conf. X-Ray Spectra Chem. Binding, Karl Marx University, Leipzig*, 1966, p. 1.
4 Alexander, J.J. and H.B. Gray, *J. Amer. Chem. Soc.*, 90 (1968) 4260.
5 Azaroff, L.V., *Rev. Mod. Phys.*, 35 (4) (1963) 1012.
6 Bagus, P.S., *Phys. Rev. A*, 139 (1965) 619.
7 Barinskii, R.L., *Zh Strukt. Khim.*, 8 (1967) 897.
8 Barinskii, R.L., *Dokl. Akad. Nauk USSR*, 83 (3) (1952) 381.
9 Barinskii, R.L. and V.I. Nefedov, *Izv. "Nauka"*, (1966).
10 Barinskii, R.L. and E. Nadzhakov, *Dokl. Bolg. Akad. Nauk*, 13 (1960) 31.
11 Barton, V.P. and G.A. Lindsay, *Phys. Rev.*, 46 (1934) 362.
12 Beaman, W.W. and M. Friedman, *Phys. Rev.*, 56 (1939) 392.
13 Beaman, W.W., J. Forss and J.N. Humphrey, *Phys. Rev.*, 67 (1945) 212.
14 Beaman, W.W. and J.A. Bearden, *Phys. Rev.*, 61 (1942) 455.
15 Becker, M.V., *Naturwissenschaften*, 51 (1964) 633.
16 Bergengren, J., *Z. Phys.*, 3 (1920) 247.
17 Best, P.E., *J. Chem. Phys.*, 47 (1967) 4002.
17a Bhat, N.V., *Acta Crystallogr., Sect. A*, 27 (1971) 71.
18 Bhide, V.G. and N.V. Bhat, *J. Chem. Phys.*, 48 (1968) 3103.
19 Bhide, V.G. and N.V. Bhat, *J. Chem. Phys.*, 50 (1969) 42.
20 Birks, L.S., *X-Ray Spectrochemical Analysis (NRL)*, (1959).
21 Boehm, G., A. Faessler and G. Rittmayer, *Z. Naturforsch. B*, 9 (1954) 509.
22 Boke, K., *Z. Phys. Chem. (Frankfurt am Main)*, 10 (1956) 45, 59; 11 (1957) 326.
23 Brummer, O. and G. Dragger, *Int. Conf. X-Ray Spectra Chem. Binding, Karl Marx University, Leipzig*, 1966, p. 35.
24 Cauchois, Y., *C.R. Acad. Sci.*, 227 (1948) 65.
25 Cauchois, Y., *Les Spectres de Rayons X et la Structure Electronique de la Matière*, Gauthier-Villars, Paris, 1948.
26 Collet, V., Contribution to the study of the nature of transition metal complexes by X-ray spectroscopy, *Thesis Doct. Sci. Phys.*, Paris, 1959, p. 52.
27 Compton, A.H. and S.K. Allison, *X-Rays in Theory and Experiment*, Van Nostrand, Princeton, New Jersey, U.S.A., 1963.
28 Coster, D., *Physica (Utrecht)*, 2 (1935) 606.
29 Coster, D., *Z. Phys.*, 25 (1924) 83.
30 Coster, D. and G.H. Klammer, *Physica (Utrecht)*, 1 (1934) 145.
31 Coster, D. and S. Kiestra, *Physica (Utrecht)*, 14 (1948) 175.
32 Cotton, F.A. and C.J. Ballhausen, *J. Chem. Phys.*, 25 (1956) 617.
33 Cotton, F.A. and H.P. Hanson, *J. Chem. Phys.*, 25 (1956) 619.
34 Cotton, F.A. and H.P. Hanson, *J. Chem. Phys.*, 28 (1958) 83.
35 Cotton, F.A. and H.P. Hanson, *J. Chem. Phys.*, 26 (1957) 1758.
36 Deodhar, G.B., *Int. Conf. X-Ray Spectra Chem. Binding, Karl Marx University, Leipzig*, 1965, p. 65.
37 Fischer, E.O., *Angew. Chem.*, 67 (1955) 455.
38 Glen, G.L. and C.G. Dod, *J. Appl. Phys.*, 39 (1968) 5372.
39 Gusatinskii, A.N. and S.A. Ischenko, *Bull. Acad. Sci. USSR, Phys. Ser.*, 31 (1967) 1017.
40 Gusatinskii, A.N. and S.A. Nemnonov, *Int. Conf. X-Ray Spectra Chem. Binding, Karl Marx University, Leipzig*, 1966, p. 124.
41 Hanson, H.P., *Develop. Appl. Spectrosc.*, 2 (1963) 254.
42 Hanson, H.P. and W.W. Beaman, *Phys. Rev.*, 76 (1949) 118.
43 Hanson, H.P. and J.R. Knight, *Phys. Rev.*, 102 (1956) 632.
44 Hartree, D.R., R. de L. Kronig and H. Peterson, *Physica (Utrecht)*, 1 (1934) 895.
45 Hayasi, T., *Sci. Rep. Tohoku Univ., Ser. 1*, 33 (1949) 123.

46 Hayasi, T., *Sci. Rep. Tohoku Univ., Ser. 1*, 33 (1949) 183.
47 Hayasi, T., *Sci. Rep. Tohoku Univ., Ser. 1*, 34 (1950) 185.
48 Hill, R. and O.R. Howell, *Phil. Mag.*, 48 (1924) 833.
49 Hofmann, *Z. Kristallogr., Kristallgeometrie, Kristallphys., Kristallchem.*, 78 (1931) 279.
50 Jørgenson, C.K., Chemical bonding from absorption spectra, *Solid State Phys.*, 13 (1962) 448.
51 Karalnik, S.M., *Bull. Acad. Sci. USSR, Phys. Ser.*, 21 (1957) 1432.
52 Kauer, E., *Z. Phys. Chem. (Frankfurt am Main)*, 6 (1956) 105.
53 Keeling, R.O., Jr., *Developments in Applied Spectroscopy*, Vol. 2, Plenum Press, New York, 1963, p. 263.
54 Kiyono, S., *Sci. Rep. Tohoku Univ., Ser. 1*, 36 (1952) 1.
55 Kiyono, S. and C. Sugawara, *Technol. Rep. Tohoku Univ.*, 30 (1965) 9.
56 Koslenkov, A.I., *Izv. Akad. Nauk USSR, Ser. Fiz.*, 25 (1961) 957.
57 Kossel, W., *Z. Phys.*, 1 (1920) 119.
58 Kostarev, A.I., *Z. Eksp. Teor. Fiz.*, 11 (1941) 60; 19 (1949) 413.
59 Kronig, R. de L., *Z. Phys.*, 70 (1931) 317; 75 (1932) 191; 75 (1932) 468.
60 Levy, R.M., *J. Chem. Phys.*, 43 (1965) 1846.
61 Lindh, A.E., *Z. Phys.*, 6 (1921) 303.
61a Lytle, F.W., *Boeing Sci. Res. Lab. Rep. D1-82-0361*, 1964.
62 Mande, C. and A.R. Chetal, *Indian J. Phys.*, 38 (1964) 433.
63 Mande, C. and A.R. Chetal, *Curr. Sci.*, 33 (1964) 707.
64 Mande, C., *Curr. Sci.*, No. 22, Nov. 20, 1966.
65 Mande, C. and A.R. Chetal, *Int. Conf. X-Ray Spectra Chem. Binding, Karl Marx University, Leipzig*, 1966, p. 194.
66 Meisel, A., *Phys. Status Solidi*, 10 (2) (1965) 365.
67 Miller, A., *Phys. Chem. Solids*, 29 (1968) 633.
68 Mishra, M.B., *D. Phil. Thesis*, Allahabad Univ., India, 1967.
69 Mishra, M.B., H.L. Nigam and A. Mehra, *J. Inorg. Nucl. Chem.*, 30 (1968) 881.
70 Mishra, M.B., H.L. Nigam and S.C. Sinha, *C.R. Acad. Bulg. Sci.*, 20 (1967) 4.
71 Mishra, M.B. and H.L. Nigam, *Acta Chim. (Budapest)*, 57 (1) (1968) 1.
72 Mitchell, G. and W.W. Beaman, *J. Chem. Phys.*, 20 (1952) 1298.
73 Mitchell, G., *J. Chem. Phys.*, 37 (1962) 216.
74 Mizuno, J., K. Ukei and J. Sugawara, *J. Phys. Soc. Jap.*, 14 (1959) 383.
75 Mookherji, T., *Indian J. Phys.*, 36 (1962) 215.
76 Mukherji, C., *D. Phil. Thesis*, Allahabad Univ., India, 1967.
77 Nemnonov, S.A., V.F. Volkov and V.S. Suetin, *Phys. Metals Metallogr. USSR*, 21 (4) (1967).
78 Nigam, A.N., *D. Phil. Thesis*, Allahabad Univ., India, 1957.
79 Nigam, A.N., personal communication, 1971 (*K*-absorption edge data on some halo complexes of niobium).
80 Nigam, H.L., R.C. Kapoor, U. Kapoor and S.C. Srivastava, *Indian J. Chem.* 3 (1965) 443.
81 Nigam, H.L. and U.C. Srivastava, *Inorg. Chim. Acta*, 5 (1971) 338.
82 Nigam, H.L. and V.K. Mathur, *Naturwissenschaften*, 25 (1964) 35.
83 Nigam, H.L. and U.C. Srivastava, *Chem. Commun.*, 14 (1971) 761.
84 Nigam, H.L. and U.C. Srivastava, *Can. J. Chem.*, 49 (1971) 3229.
85 Nigam, H.L. and U.C. Srivastava, *Z. Naturforsch.*, 266 (10) (1971) 997.
86 Nigam, H.L. and S.C. Sinha, *Curr. Sci.*, 35 (1966) 63.
87 Nigam, H.L. and S.C. Sinha, *Indian J. Chem.*, 5 (3) (1967) 117.
88 Obashi, M. and T. Nakamura, *Jap. J. Appl. Phys.*, 10 (10) (1971) 1437.
89 Obashi, M., *Sci. Rep. Osaka Univ.*, 10 (1961) 17.
90 Obashi, M., *Sci. Rep. Osaka Univ.*, 6 (1957) 65; 7 (1958) 35.
91 Obashi, M. and M. Nakamori, *Sci. Rep. Osaka Univ.*, 8 (1959) 35.
91a Obashi, M. and T. Nakamora, *Jap. J. Appl. Phys.*, 10 (1971) 1437.
92 Obashi, M., *Sci. Rep. Osaka Univ.*, 16 (1) (1967) 1.
93 Orgel, L.E., *J. Chem. Phys.*, 23 (1955) 1004.

94 Ovsyannikova, I.A., S.S. Batsanov, L.I. Nasonova, L.R. Batsanova and E.A. Nakrasov, *Bull. Acad. Sci. USSR, Phys. Ser.* 31 (1967) 936.
95 Padalia, B.D. and C.S. Gupta, Letter in *Curr. Sci.*, No. 20, (1969) 490.
96 Padalia, B.D. and V. Krishnan, *Indian J. Pure Appl. Phys.*, 9 (10) (1971) 813.
97 Paigankar, A., *Ph. D. Thesis*, Bombay Univ., 1968.
98 Pandey, K.B. and H.L. Nigam, *Indian J. Chem.*, 8 (1970) 454.
99 Pandey, K.B. and H.L. Nigam, *Proc. Chem. Symp. (Chandigarh, India)*, 1 (1969) 147.
100 Parratt, L.G., *Phys. Rev.*, 56 (1939) 295.
101 Penney, W.G., *Trans. Faraday Soc.*, 36 (1940) 627.
102 Powell, H.M. and A.F. Wells, *J. Chem. Soc., London*, (1935) 359.
103 Sandstrom, A.E., *Handbuch der Physik*, Springer-Verlag; Berlin, 1957.
104 Sanner, V.H., *Thesis*, Uppsala Univ., Sweden, 1941.
105 Sawada, M., K. Tsutsumi and A. Hayasi, *J. Phys. Soc. Jap.*, 12 (1957) 628.
106 Sawada, M., K. Tsutsumi, T. Shiraiwa, T. Ishimura and M. Obashi, *Annu. Rep. Sci. Works, Fac. Sci., Osaka Univ.*, 7 (1969) 1.
107 Schuette, K.W., *Thesis, Tulsa Univ.*, 1965.
108 Seka, W. and H.P. Hanson, *J. Chem. Phys.*, 50 (1969) 344.
109 Shiraiwa, T., T. Ishimura and M. Sawada, *J. Phys. Soc. Jap.*, 13 (1958) 847.
110 Sinha, K.P. and C. Mande, *Indian J. Phys.*, 37 (1963) 257.
111 Srivastava, U.C., K.B. Pandey and H.L. Nigam, *Indian J. Chem.*, in press.
112 Srivastava, U.C. and H.L. Nigam, *Indian J. Chem.*, 9 (1971) 1301.
113 Srivastava, U.C., H.L. Nigam and A.N. Vishnoi, *Indian J. Pure Appl. Phys.*, 9 (1971) 63.
114 Srivastava, U.C., H.L. Nigam and A.N. Vishnoi, *Indian J. Pure Appl. Phys.*, 10 (1972) 61.
115 Srivastava, U.C., H.L. Nigam and A.N. Vishnoi, *Curr. Sci.*, 41 (1972) 251.
116 Srivastava, U.C. and H.L. Nigam, *Curr. Sci.*, 41 (1) (1972) 18.
117 Srivastava, U.C. and H.L. Nigam, *Indian J. Chem.*, in press.
118 Stelling, O., *Z. Phys. Chem.*, 7 (1930) 210.
119 Stelling, O., *Z. Phys.*, 50 (1928) 506.
120 Sugiura, C., *Sci. Rep. Tohoku Univ.*, 45 (1961) 248.
121 Tsutsumi, K., A. Hayase and M. Savada, *J. Phys. Soc. Jap.*, 12 (1957) 793.
122 Tsutsumi, K., *J. Phys. Soc. Jap.*, 13 (1958) 586.
123 Vainshtein, E., R.M. Ovrutskaya, B.I. Kotlyar and U.R. Linde, *Sov. Phys. – Solid State*, 5 (1964) 2150.
124 Vainshtein, E., *Dokl. Akad. Nauk USSR*, 69 (1949) 771.
125 Vainshtein, E., R.L. Barinskii and K.I. Narbut, *Zh. Eksp. Teor. Fiz.*, 23 (1952) 593.
126 Vainshtein, E., E.A. Shurakowski and I.B. Stari, *Zh. Neorg. Khim.*, 4 (1959) 245.
127 Van Nordstrand, R.A., *Handbook of X-Rays*, McGraw-Hill, New York, 1966.
128 Van Nordstrand, R.A., *Advan. Catal. Relat. Subj.*, 12 (1960) 149.
129 Van Nordstrand, R.A., *Conference on Non-Crystalline Solids*, Wiley, New York, 1960.
130 Van Nordstrand, R.A., *Int. Conf. X-Ray Spectra Chem. Binding, Karl Marx University, Leipzig*, 1966 p. 255.
131 Van Nordstrand, R.A., K.W. Schuette and R.D. Hartmann, *Meet. Phys. X-Ray Spectra, June 1965, Ithaca.*
132 Van Nordstrand, *Amer. Chem. Soc., Div. Petrol. Chem.*, 46 (1959) 183.
133 Verma, L.P. and B.K. Agarwal, *J. Phys. C*, 1 (1968) 1658.
134 Vishnoi, A.N., *J. Phys. C, Metal Phys. Suppl.*, 2 (1970) S227.
135 Yoshida, S., *Sci. Pap. Inst. Phys. Chem. Res., Tokyo*, 38 (1941) 272.

APPENDIX

TABLE A

X-ray *K*-absorption studies on complexes of first transition series metals

Compound	Observations relating to	Conclusions relating to	References
Chromium			
K_2CrO_4	Edge structure, low energy abs., fine structure	Hybrid (sd^3), tetrahedral, eff. charge on metal	10, 29, 42, 89, 104, 128, 129
$K_2Cr_2O_7$			29, 42, 89, 104
$Cr(CO)_4$	Fine structure	Eff. charge on metal	7
$Cr(CO)_6$	Edge structure, low energy abs., fine structure	Bonding assignments, eff. charge on metal	10, 35, 52
$Na_3Cr(C_2O_4)_3$			35
$[Cr(NH_3)_6](NO_3)_3$ $[Cr(en)_3](NCS)_3$ *trans*-$NH_4[Cr(NH_3)_2(NCS)_4]$ $K_3Cr(NCS)_6$ *trans*-$[Cr(en)_2(NCS)_2]NCS$	Additivity of fine structure due to different ligands	Coordination symmetry, technique applicable to the study of mixed-ligand complexes	128–130
$Cr(en)_3(NCS)_3$	Low energy abs. edge structure	Type of (*cis–trans*) isomer	108
$K_3Cr(CN)_6$ Na_2CrO_4 $KCrO_3Cl$ $K_3Cr(NCS)_6$	Edge structure	Coordination symmetry, agreement with MO theory predictions	108
Manganese			
$Mn(aq.)^{++}$	Edge shape	Character of aquated trans. metal ions	42
$KMnO_4$	Edge shape, low energy abs., fine structure	Coord. symm., tet., eff. charge on metal	7, 29, 42, 89, 104, 110, 128–130
$CoMn_2O_4$	Spectral shift, additivity of edge structure	Valency of metal ion mixed stereochemistry	123
$K_3Mn(CN)_6$	Edge shape (character of oct. complexes involving linear ligands), fine structure	Coord. symm., eff. charge on metal	7, 110, 128, 129
$K_4Mn(CN)_6$	Fine structure	Coord. symm., hybridization	89

TABLE A (cont'd)

Compound	Observations relating to	Conclusions relating to	References
$C_5H_5Mn(CO)_3$	Fine structure	Eff. charge on metal	7
$Mn(C_5H_7O_2)_2.2H_2O$ $Mn(C_5H_7O_2)_3$	Edge structure, shift of *K*-abs. max.	Coord. symm., dependence on oxid. state	38
Iron			
$Fe(phen)_3(ClO_4)_2$ $Fe(phen)_2(ClO_4)_3$ $Fe(dipy)_3(ClO_4)_2$ $Fe(dipy)_3(ClO_4)_3$ $Fe(dipy)_2(CN)_2.3H_2O$ $Fe(phen)_2(CN)_2$ $Fe(5\text{-}N\text{-}phen)_3(ClO_4)_2$ $Fe(5\text{-}Cl\text{-}phen)_3(ClO_4)_2$ $Fe(5\text{-}Br\text{-}phen)(ClO_4)_2$ $Na_4Fe(CN)_6$ $Fe(2Cl.phen)_3(ClO_4)_2$ $Fe(phen)_2Cl_2$ $Fe(phen)_2Br_2$ $Fe(phen)_2(N_3)_2$ $Fe(phen)_2(SCN)_2$ $Fe(phen)_2(SeCN)_2$ $FeSO_4.7H_2O$ $FeCl_2.4H_2O$	Edge structure, $a^*_{1g}-t^*_{1u}$ energy separation measured	Type of isomer, relation of the energy separation to spectrochemical series	108
$K_3Fe(CN)_6$	Fine structure, low energy abs., edge structure	Bonding, eff. charge on metal, bonding assignments, coord. symm.	10, 35, 38, 89, 128, 129
$K_4Fe(CN)_6$	Edge shape, fine structure	Bonding, hybridization, coord. symm.	38, 42, 128, 129
$Co_2Fe(CN)_6$ $Fe_4[Fe(CN)_6]_3$	Edge structure, fine structure	Determination of lattice sites	38
$Na_2[Fe(CN)_5NO]2H_2O$	Edge structure, fine structure	Bonding, relation to MO levels	35, 38
$Fe(CO)_5$	Fine structure	Eff. charge on metal	10
Cobalt			
Vitamin B_{12}	*K* edge shift	Valency of metal ion	21
$Co(aq)^{++}$ (pink)	Edge structure	Oct. coord.	36
$Co(aq)^{++}$ (blue)	Edge structure	Tet. coord.	36
$Na_3[Co(NO_2)_6]$ $[Co(H_2O)_6]Cl_2$ Co–oxinate dihydrate	*K* edge shifts, edge structure, fine structure	Valency of metal ion, coord. symm. hybrid., MO bonding *config.*,	63–65, 68

TABLE A (cont'd)

Compound	Observations relating to	Conclusions relating to	References
Co–oxinate (anhyd.) Co^{II}–α-bis-pyr. chloride		relation to magnetic data, bond length determination	
Co^{II}–β-bis-pyr. chloride Diquinol.Co^{II} chloride Co–thiomalic acid (TMA)			
$[Co(en)_3]Cl_3$ $(NH_4)_3[Co(NO_2)_6]$	Edge structure, low energy abs.	Transition assignments	35
$Co(C_5H_7O_2)_2$	Relative energy of *K*-abs. max., fine structure	Valency of the metal ion, eff. charge on metal	7, 8, 38
$Co(NH_3)_6^{2+}$	Splitting of *K*-abs. max.	*p*-orbital splitting	34
$K_3Co(CN)_6$ $[Co(NH_3)_6]Cl_3$ $Co(en)_3(ClO_4)_3$	Fine structure	Coord. symm., hybridization	89
$Fe[Co(CN)_6]$	Fine structure	Determination of lattice sites	38
$Co[(et)_4dien]Br_2$ $Co[(et)_4dien](NCS)_2$ $Co[(et)_4dien](N_3)_2$	Relative shift of *K*-abs. max.; splitting and broadening of main peak	MO energy level correlations, influence of nature of ligand and metal–ligand bond	38
$Fe^{3+}[Co^{2+}Fe^{3+}]O_4$ $Ge[Co_2]O_4$ $Co[Al_2]O_4$ $Co[Cr_2]O_4$ $Co[Mn_2]O_4$	Edge width (EW)	Coordination symmetry around cobalt in lattice sites; EW (tet.) > EW (oct.)	
Co^{II}–bis-ethyl-1-amidino-2-thiourea Co^{III}–isonitroso-acetyl acetonate	*K*-edge shifts, energy of *K*-abs. max., edge structure	Valency of metal ion, coord. symm., transition assignments	2
$Co^{III}(INAP)_3$	Edge structure	Coord. symm. oct.	95
$Co^{II}(DPDTP)_2$	Edge splitting	$1s \rightarrow 4p$ and $1s \rightarrow 5p$	96
$Co^{III}(INAP)_3$	Monotonic edge	Coord. symm. oct.	96
Co^{III}–acetyl acetonate	Energy of *K*-abs. max., edge structure	Transition assignments	22
$Co_2(CO)_8$	Edge fine structure	Spectra – character of bridging bonds	22, 132
Nickel Ni^{++}(aq.)	Edge structure	Coord. symm.	14, 24, 35, 41, 43
$Ni(CN)_4^{2-}$	Edge structure, low energy abs.	Hybrid. (dsp^2), coord. symm.	37, 72, 73, 89, 124

TABLE A (cont'd)

Compound	Observations relating to	Conclusions relating to	References
$Ni(NH_3)_6^{2+}$	Splitting of *K*-abs. max.	Ligand field theory inapplicable to *p*-orbital splitting[49]	35, 52
Ni^{II}–bis-salicylaldehyde	Edge structure	Coord. symm.,	35
$[Ni(NH_3)_6]Br_2$	low energy abs.	transition assignments	
$Ni(en)_3(NO_3)_2$		to antibonding MO	
$[Ni(NH_3)_4(H_2O)_2](NO_3)_2$		levels	
$Ni(en)_2(NO_2)Cl$	Fine structure	Eff. charge on metal	7
Ni^{II}–bis-ethyl-1-amidino-2-thiourea (ATU)	Edge structure, energy of *K*-abs. max.	Transition assignments, coord. symm.	100
$Ni(NO_3)_2.6H_2O$	Edge structure	MO explanation	108
$[Ni(NH_3)_6]Cl_2$	Fine structure	Coord. symm.	92
$K_2[Ni(CN)_4]$			
Copper			
$Cu(aq.)^{2+}$	Edge shape (monotonic edge)	Coord. symm. (oct.)	14, 33
$Cu(NH_3)_4^{2+}$ (aq.)	Edge structure, edge width, edge shifts, splitting of *K*-abs. max.	Coord. symm., calculation of edge shift from optical data (a cycle)	14, 33, 91a
$Cu_2(CN)_4^{2-}$ (aq.)	Edge structure	Coord. symm.	14
$Cu(proline)_2.2H_2O$	Splitting and	Support to ligand	33
$Cu(en)_2(NO_3)_2$	broadening of	field correlation	
$Cu(NH_3)_4SO_4.H_2O$	*K*-abs. max., small	of *p*-orbital splitting[49],	
$[Cu(NH_3)_4](NO_3)_2$	maxima at ~10 eV below main peak	transition assignments	
Cu–formate tetrahydrate	Fine structure	Nature of coordination sphere	106
$Cu(C_2H_4NO_2)_2.xH_2O$ (bis-glycino copper hydrate)			
Cu-phthalocyanine α-form			
Cu-phthalocyanine β-form			
$CuMn_2O_4$	*K* edge shift	Valency of metal ion	67
$Cu_2Fe(CN)_6$	*K* edge shift	Valency of metal ion	133
$Cu_2(CH_3COO)_4.2H_2O$	*K* edge shift	Correlation with	133, 91a,
$K[CuF_3]$		metal–metal bond	58
$Cu^{I}(bipy)_2ClO_4$	Fine structure	Fine structure	91a
Cu(acac)–$(OH_2)_2$.P			
Zinc			
$Zn(aq.)^{2+}$	Edge shape	Character of hexa-aquated trans. metal ions	14, 24, 34, 41, 43
$Zn(NH_3)_4^{2+}$ (aq.)	Splitting of *K*-abs. max.	Correlation with theory[16]	34
$[Zn(en)_3]SO_4$	No splitting of	Narrow abs. line	34

TABLE A (cont'd)

Compound	Observations relating to	Conclusions relating to	References
$[Zn(H_2O)_6](BrO_3)_2$ $[Zn(H_2O)_6](ClO_4)_2$ $Zn(proline)_2$ $Zn(glycine)_2.2H_2O$ Zn–oxinate (anhyd.) Zn–oxinate (dihydrate) $Zn(C_2H_3O_2)_2.2H_2O$ $Zn(ac.ac.)_2$	*K*-abs. max., broadening in some cases, relative shifts in *K*-abs. max.	related to completely filled 3*d*, coord. symm.	
$Zn(NH_3)_3Cl_5$ $Zn(C_5H_7O_2)$ $Zn(C_6H_5)_2$	Fine structure	Eff. charge on metal	7

TABLE B

X-ray *K* and L_{III} absorption studies on complexes of second transition series metals

Compound	Observations related to	Conclusions related to	References
Yttrium (K-)			
Y^{3+} (aq.) Y–(mono, di and tri) chloroacetates Y–maleate Y–succinate	*K* edge shifts (w.r.t. Y_2O_3) edge structure, fine structure	Spectral character of Y^{3+} ions, edge shifts decrease with increase of covalency, *K*-abs. max. due to $1s \rightarrow 5p$, shift in *K*-abs. max.	18
Y–chromate Y–vanadate	Shape of the abs. edge	Tetrahedral coordination symmetry of yttrium	17a
Niobium (K-)			
$K_2NbO_2F_5$ $K_2NbOF_5.H_2O$ Na_3NbOF_6 $(NH_4)_2NbOF_5$ $(NH_4)_3NbOF_6$ $(NH_4)_3NbOF_6$ $CsNbF_6$	Edge structure, edge shifts, edge widths	Coord. symm. nature of metal–nearest neighbour interactions	79
Molybdenum (L_{III})			
$K_4Mo(CN)_8$ $(NH_4)_3MoO_4$	F ne structure, edge structure	Transition assignments	7

TABLE C

L_{III} absorption studies of some third transition series metal complexes

Compound	Observations relating to	Conclusions relating to	References
Platinum			
$[Pt(NH_2OH)_4]^{2+}$ $[Pt(CN)_4]^{2-}$ $[Pt(SO_3)_4]^{6-}$ $[Pt(SCN)_4]^{2-}$ $[PtCl_4]^{2-}$ $[Pt(OH_6]^{2-}$ $[PtCl_6]^{2-}$	X-ray band shifts ($2p_{3/2} \rightarrow 5d$)	Comparison with optical *d*-shell transitions	26
K_2PtCl_4 $(NH_4)_2PtCl_4$ Na_2PtCl_6 K_2PtCl_6 $(NH_4)_2PtCl_6$ $MgPt(CN)_6$ $K_2Pt(CN)_6$ $Na_2Pt(CN)_6$	Edge shifts	Transition assignments, electronic configurations	36, 78
Gold			
$MAuCl_4$ (M = Na, K, H, NH_4) $KAuBr_4$ $KAuI_4$	Edge shifts	Transition assignments, electronic configurations	36, 78

TABLE D

Miscellaneous

Compound	Observations relating to	Conclusions relating to	References
TiO_2	Splitting of low energy abs. and of the main peak	Splitting of 3*d* orbitals (ligand field effect), relation to MO energy level diagram	3, 126
$(NH_4)_3InF_6$	Edge structure, low energy abs.	Nature of coordination sphere	40
Some Ni and Co complexes	*K*-abs. spectra		26
Re^{IV} complexes	L_{III}-abs. spectra		26